Supporting material (Appendix) for the thesis:

The analysis of high-throughput biological datasets utilising distributed computing

Submitted by

Jamie J. Alnasir

Supervisor: Hugh P. Shanahan

Advisor: Gregory Z. Gutin

2017

Appendix 1

Testing the Protein Databank (Chapter 5)

1.1 PDB-Hadoop concatenation procedure *cnvpdb*

The concatenation procedure *cnvpdb* for producing a single file from many PDB files, for upload to HDFS is listed below:

Algorithm 1: The concatenation process is achieved by replacing standard EOL (End of Line) control characters in each original PDB file, which delimit PDB records by line, with a custom delimiter. The result is a set of tuples P' in the form $\langle p_1, p_2, ..., p_N \rangle$, in which each PDB macromolecular structure is represented by a single string v containing the custom delimiter.

1 function *cnvpdb*(P);
  Input : Set of Protein Databank (PDB) files P
  Output: Set of tuples P' in the form $\langle p_1, p_2, ..., p_N \rangle$, the concatenated PDB entries
2 $CRLF \leftarrow$ #13#10; *// ASCII codes for CRLF EOL (End of Line) delimiter*
3 $CD \leftarrow$ "^|"; *// Our custom delimiter*
4 **for** *each* $p \in P$ **do**
5 $L \leftarrow |p|$; *// obtain record length of PDB file p*
6 $k \leftarrow p[0]$; *// extract PDB-ID from first line of PDB file p*
7 $pdbData \leftarrow p[1..L]$; *// extract PDB record data from PDB file p*
8 $v \leftarrow$ replace all instances of $CRLF$ in $pdbData$ with CD;
9 append $\langle k, v \rangle$ to P';
10 **end**
11 Return P';

1.2 Running the user analysis job

The execution of PDB-Hadoop is outlined in Figure 5.1 in chapter 5 of the thesis. The user's *analysis program* and optional *post-processing* are executed in a *map* step using Hadoop streaming. Scheduling of the tasks is carried out using YARN (Yet Another Resource Negotiator) which is standard as of Apache Hadoop V2.0.

Prior to running an analysis job with PDB-Hadoop, the concatenation procedure *cnvpdb* is used to generate a single file containing multiple PDB entries on which to perform analyses on for upload to HDFS. *cnvpdb*, which is implemented as a bash script, is applied to a set of PDB files P which can comprise the whole of the Protein Databank (approximately 100 GB[1] as of January 2017) or a subset thereof, to produce the single file P'.

Additionally, the path to the user analysis program must be specified within the configuration, which also provides other configurable options, these are listed in Table 1.1 below:

Parameter	Purpose
*_LEGACY_PROGRAM_	Specifies the path to the program to execute in parallel fashion on Hadoop.
_TEMP_FOLDER_	Designates a temporary folder (default "/tmp"), which must be writable to YARN (i.e. the Hadoop user).
_POST_PROC_PROGRAM_	Specifies path to the user's post-processing program that takes output from the execution of user program (defined above) and performs textual processing on the results.
_MAX_PDB_SIZE_	If set PDB-Hadoop ignores processing of files greater than specified size (in bytes)

Table 1.1: Configuration parameters for PDB-Hadoop. * Specifying the path to the legacy job is obligatory, all other parameters are optional.

Initiation of a PDB-Hadoop analysis job is achieved by running the Hadoop streaming jar, specifying the path to the PDD-Hadoop external *mapper* script, as follows:

As discussed in chapter 2 (section 2.4.2), when MapReduce jobs are submitted to Hadoop, the input data file is partitioned into *splits* which are input to the *map* and/or *reduce* functions in the MapReduce job. Consequently Hadoop stores the results of MapReduce jobs on HDFS as a directory containing the job output files that correspond to the input splits created by Hadoop when the job was submitted. When a PDB-Hadoop job is executed, the input file of PDB entries P' will therefore be partitioned into *splits* and the resulting output files stored in HDFS. The results of the analysis, to which the users *post-processing* may have already been applied, can be obtained as a single file using Hadoop's *getmerge* command which concatenates multiple split output into a single file.

[1] for all PDB files of *.ent* extension and excluding the same entries in other formats, such as *.xml*.

```
hadoop jar /usr/lib/hadoop-mapreduce/hadoop-streaming.jar \
-Dmapred.sort.avoidance=0 \
-Dmapred.reduce.tasks=0 \
-D stream.non.zero.exit.status.is.failure=false \
-input  /user/hduser/pdb-text-full.txt
-output /user/hduser/pdb-legacy-output \
-mapper "/path/to/local/pdb-hadoop/pdb-hadoop.sh" \
```

Figure 1.1: A PDB-Hadoop job is initiated by executing the Hadoop streaming jar with path parameters. These are the path to the PDB-Hadoop external *mapper* executable (on the local file system) together with the HDFS paths to the input data (concatenated file of PDB entries P') and destination output data (results of the *user analysis program* and any *post-processing* applied). NB: The specific paths may vary depending on the local configuration of the Hadoop cluster on which the program is run.

1.3 PDB file accessions used for benchmarking

Data used from the Protein Databank for benchmarking PDB-Hadoop (chapter 5 section 5.6) is listed below, by PDB entry (accession):

```
pdb1a30, pdb1a31, pdb1a32, pdb1a33, pdb1a34, pdb1a35, pdb1a36, pdb1a37, pdb1a38,
pdb1a39, pdb1a3a, pdb1a3b, pdb1a3c, pdb1a3d, pdb1a3e, pdb1a3f, pdb1a3g, pdb1a3h,
pdb1a3i, pdb1a3j, pdb1a3k, pdb1a3l, pdb1a3m, pdb1a3n, pdb1a3o, pdb1a3p, pdb1a3q,
pdb1a3r, pdb1a3s, pdb1a3t, pdb1a3u, pdb1a3v, pdb1a3w, pdb1a3x, pdb1a3y, pdb1a3z,
pdb1dk0, pdb1dk1, pdb1dk2, pdb1dk3, pdb1dk4, pdb1dk5, pdb1dk6, pdb1dk7, pdb1dk8,
pdb1dk9, pdb1dka, pdb1dkc, pdb1dkd, pdb1dke, pdb1dkf, pdb1dkg, pdb1dkh, pdb1dki,
pdb1dkj, pdb1dkk, pdb1dkl, pdb1dkm, pdb1dkn, pdb1dko, pdb1dkp, pdb1dkq, pdb1dkr,
pdb1dks, pdb1dkt, pdb1dku, pdb1dkw, pdb1dkx, pdb1dky, pdb1dkz, pdb1e50, pdb1e51,
pdb1e52, pdb1e54, pdb1e55, pdb1e56, pdb1e57, pdb1e58, pdb1e59, pdb1e5a, pdb1e5b,
pdb1e5c, pdb1e5d, pdb1e5e, pdb1e5f, pdb1e5g, pdb1e5h, pdb1e5i, pdb1e5j, pdb1e5k,
pdb1e5l, pdb1e5m, pdb1e5n, pdb1e5o, pdb1e5p, pdb1e5q, pdb1e5r, pdb1e5s, pdb1e5t,
pdb1e5u, pdb1e5v, pdb1e5w, pdb1e5x, pdb1e5y, pdb1e5z, pdb1ef0, pdb1ef1, pdb1ef2,
pdb1ef3, pdb1ef4, pdb1ef5, pdb1ef7, pdb1ef8, pdb1ef9, pdb1efa, pdb1efc, pdb1efd,
pdb1efe, pdb1efg, pdb1efh, pdb1efi, pdb1efk, pdb1efl, pdb1efm, pdb1efn, pdb1efo,
pdb1efp, pdb1efq, pdb1efr, pdb1efs, pdb1eft, pdb1efu, pdb1efv, pdb1efw, pdb1efx,
pdb1efy, pdb1efz, pdb1fj0, pdb1fj1, pdb1fj2, pdb1fj3, pdb1fj4, pdb1fj5, pdb1fj6,
pdb1fj7, pdb1fj8, pdb1fj9, pdb1fja, pdb1fjb, pdb1fjc, pdb1fjd, pdb1fje, pdb1fjg,
pdb1fjh, pdb1fjj, pdb1fjk, pdb1fjl, pdb1fjm, pdb1fjn, pdb1fjo, pdb1fjp, pdb1fjq,
pdb1fjr, pdb1fjs, pdb1fjt, pdb1fju, pdb1fjv, pdb1fjw, pdb1fjx, pdb1fp0, pdb1fp1,
pdb1fp2, pdb1fp3, pdb1fp4, pdb1fp5, pdb1fp6, pdb1fp7, pdb1fp8, pdb1fp9, pdb1fpb,
pdb1fpc, pdb1fpd, pdb1fpe, pdb1fpf, pdb1fpg, pdb1fph, pdb1fpi, pdb1fpj, pdb1fpk,
pdb1fpl, pdb1fpm, pdb1fpn, pdb1fpo, pdb1fpp, pdb1fpq, pdb1fpr, pdb1fps, pdb1fpt,
pdb1fpu, pdb1fpv, pdb1fpw, pdb1fpx, pdb1fpy, pdb1fpz, pdb1ga0, pdb1ga1, pdb1ga2,
pdb1ga3, pdb1ga4, pdb1ga5, pdb1ga6, pdb1ga7, pdb1ga8, pdb1ga9, pdb1gab, pdb1gac,
pdb1gad, pdb1gae, pdb1gaf, pdb1gag, pdb1gah, pdb1gai, pdb1gaj, pdb1gak, pdb1gal,
pdb1gam, pdb1gan, pdb1gao, pdb1gaq, pdb1gar, pdb1gat, pdb1gau, pdb1gav, pdb1gaw,
pdb1gax, pdb1gay, pdb1gaz, pdb1uq4, pdb1uq5, pdb1uqa, pdb1uqb, pdb1uqc, pdb1uqd,
pdb1uqe, pdb1uqf, pdb1uqg, pdb1uqr, pdb1uqs, pdb1uqt, pdb1uqu, pdb1uqv, pdb1uqw,
pdb1uqx, pdb1uqy, pdb1uqz, pdb2a30, pdb2a31, pdb2a32, pdb2a33, pdb2a35, pdb2a36,
```

pdb2a37, pdb2a38, pdb2a39, pdb2a3a, pdb2a3b, pdb2a3c, pdb2a3d, pdb2a3e, pdb2a3f,
pdb2a3g, pdb2a3h, pdb2a3i, pdb2a3j, pdb2a3k, pdb2a3l, pdb2a3m, pdb2a3n, pdb2a3p,
pdb2a3q, pdb2a3r, pdb2a3s, pdb2a3t, pdb2a3u, pdb2a3v, pdb2a3w, pdb2a3x, pdb2a3y,
pdb2a3z, pdb2dk1, pdb2dk2, pdb2dk3, pdb2dk4, pdb2dk5, pdb2dk6, pdb2dk7, pdb2dk8,
pdb2dk9, pdb2dka, pdb2dkb, pdb2dkc, pdb2dkd, pdb2dke, pdb2dkf, pdb2dkg, pdb2dkh,
pdb2dki, pdb2dkj, pdb2dkk, pdb2dkl, pdb2dkm, pdb2dkn, pdb2dko, pdb2dkp, pdb2dkq,
pdb2dkr, pdb2dks, pdb2dkt, pdb2dku, pdb2dkv, pdb2dkw, pdb2dkx, pdb2dky, pdb2dkz,
pdb2e50, pdb2e51, pdb2e52, pdb2e53, pdb2e54, pdb2e55, pdb2e56, pdb2e59, pdb2e5a,
pdb2e5b, pdb2e5c, pdb2e5d, pdb2e5e, pdb2e5f, pdb2e5g, pdb2e5h, pdb2e5i, pdb2e5j,
pdb2e5k, pdb2e5l, pdb2e5m, pdb2e5n, pdb2e5o, pdb2e5p, pdb2e5q, pdb2e5r, pdb2e5s,
pdb2e5t, pdb2e5u, pdb2e5v, pdb2e5w, pdb2e5x, pdb2e5y, pdb2e5z, pdb2ef0, pdb2ef1,
pdb2ef2, pdb2ef4, pdb2ef5, pdb2ef6, pdb2ef7, pdb2ef8, pdb2ef9, pdb2efa, pdb2efb,
pdb2efc, pdb2efd, pdb2efe, pdb2eff, pdb2efg, pdb2efh, pdb2efi, pdb2efj, pdb2efk,
pdb2efl, pdb2efn, pdb2efo, pdb2efp, pdb2efq, pdb2efr, pdb2efs, pdb2eft, pdb2efu,
pdb2efv, pdb2efw, pdb2efx, pdb2efy, pdb2efz, pdb2fj0, pdb2fj1, pdb2fj2, pdb2fj3,
pdb2fj4, pdb2fj5, pdb2fj6, pdb2fj7, pdb2fj8, pdb2fj9, pdb2fja, pdb2fjb, pdb2fjc,
pdb2fjd, pdb2fje, pdb2fjf, pdb2fjg, pdb2fjh, pdb2fji, pdb2fjk, pdb2fjl, pdb2fjm,
pdb2fjn, pdb2fjp, pdb2fjr, pdb2fjs, pdb2fjt, pdb2fju, pdb2fjv, pdb2fjw, pdb2fjx,
pdb2fjy, pdb2fjz, pdb2fp0, pdb2fp1, pdb2fp2, pdb2fp3, pdb2fp4, pdb2fp7, pdb2fp8,
pdb2fp9, pdb2fpb, pdb2fpc, pdb2fpd, pdb2fpe, pdb2fpf, pdb2fpg, pdb2fph, pdb2fpi,
pdb2fpk, pdb2fpl, pdb2fpm, pdb2fpn, pdb2fpo, pdb2fpp, pdb2fpq, pdb2fpr, pdb2fps,
pdb2fpt, pdb2fpu, pdb2fpv, pdb2fpw, pdb2fpx, pdb2fpy, pdb2fpz, pdb2ga0, pdb2ga1,
pdb2ga2, pdb2ga3, pdb2ga4, pdb2ga5, pdb2ga6, pdb2ga7, pdb2ga8, pdb2ga9, pdb2gaa,
pdb2gab, pdb2gac, pdb2gae, pdb2gaf, pdb2gag, pdb2gah, pdb2gai, pdb2gaj, pdb2gak,
pdb2gal, pdb2gam, pdb2gan, pdb2gao, pdb2gaq, pdb2gar, pdb2gas, pdb2gat, pdb2gau,
pdb2gaw, pdb2gax, pdb2gaz, pdb3a30, pdb3a31, pdb3a32, pdb3a33, pdb3a34, pdb3a35,
pdb3a36, pdb3a37, pdb3a38, pdb3a39, pdb3a3a, pdb3a3b, pdb3a3c, pdb3a3d, pdb3a3e,
pdb3a3f, pdb3a3g, pdb3a3h, pdb3a3i, pdb3a3j, pdb3a3k, pdb3a3n, pdb3a3o, pdb3a3p,
pdb3a3q, pdb3a3r, pdb3a3t, pdb3a3u, pdb3a3v, pdb3a3w, pdb3a3x, pdb3a3y, pdb3a3z,
pdb3dk0, pdb3dk1, pdb3dk2, pdb3dk3, pdb3dk4, pdb3dk5, pdb3dk6, pdb3dk7, pdb3dk8,
pdb3dk9, pdb3dka, pdb3dkb, pdb3dkc, pdb3dkd, pdb3dke, pdb3dkf, pdb3dkg, pdb3dkh,
pdb3dki, pdb3dkj, pdb3dkk, pdb3dkl, pdb3dkm, pdb3dkn, pdb3dko, pdb3dkp, pdb3dkq,
pdb3dkr, pdb3dks, pdb3dkt, pdb3dku, pdb3dkv, pdb3dkw, pdb3dkx, pdb3dky, pdb3dkz,
pdb3e50, pdb3e51, pdb3e53, pdb3e54, pdb3e55, pdb3e56, pdb3e57, pdb3e58, pdb3e59,
pdb3e5a, pdb3e5b, pdb3e5c, pdb3e5d, pdb3e5e, pdb3e5f, pdb3e5h, pdb3e5i, pdb3e5j,
pdb3e5k, pdb3e5l, pdb3e5m, pdb3e5n, pdb3e5o, pdb3e5p, pdb3e5q, pdb3e5r, pdb3e5s,
pdb3e5t, pdb3e5u, pdb3e5v, pdb3e5w, pdb3e5x, pdb3e5y, pdb3e5z, pdb3ef0, pdb3ef1,
pdb3ef2, pdb3ef3, pdb3ef4, pdb3ef5, pdb3ef6, pdb3ef7, pdb3ef8, pdb3ef9, pdb3efa,
pdb3efb, pdb3efc, pdb3efd, pdb3efe, pdb3eff, pdb3efg, pdb3efh, pdb3efi, pdb3efj,
pdb3efk, pdb3efl, pdb3efm, pdb3efo, pdb3efp, pdb3efq, pdb3efr, pdb3efs, pdb3eft,
pdb3efu, pdb3efv, pdb3efw, pdb3efx, pdb3efy, pdb3efz, pdb3fj1, pdb3fj2, pdb3fj4,
pdb3fj5, pdb3fj6, pdb3fj7, pdb3fj8, pdb3fj9, pdb3fja, pdb3fjb, pdb3fjc, pdb3fjd,
pdb3fje, pdb3fjf, pdb3fjg, pdb3fjh, pdb3fji, pdb3fjj, pdb3fjk, pdb3fjl, pdb3fjm,
pdb3fjn, pdb3fjo, pdb3fjp, pdb3fjq, pdb3fjs, pdb3fjt, pdb3fju, pdb3fjv, pdb3fjw,
pdb3fjx, pdb3fjy, pdb3fjz, pdb3fp0, pdb3fp2, pdb3fp3, pdb3fp4, pdb3fp5, pdb3fp6,
pdb3fp7, pdb3fp8, pdb3fp9, pdb3fpa, pdb3fpb, pdb3fpc, pdb3fpd, pdb3fpe, pdb3fpf,
pdb3fpg, pdb3fph, pdb3fpi, pdb3fpj, pdb3fpk, pdb3fpl, pdb3fpm, pdb3fpn, pdb3fpo,
pdb3fpp, pdb3fpq, pdb3fpr, pdb3fps, pdb3fpt, pdb3fpu, pdb3fpv, pdb3fpw, pdb3fpx,
pdb3fpy, pdb3fpz, pdb3ga0, pdb3ga1, pdb3ga2, pdb3ga3, pdb3ga4, pdb3ga5, pdb3ga6,
pdb3ga7, pdb3ga8, pdb3ga9, pdb3gaa, pdb3gab, pdb3gac, pdb3gad, pdb3gae, pdb3gaf,
pdb3gag, pdb3gah, pdb3gai, pdb3gaj, pdb3gak, pdb3gal, pdb3gam, pdb3gan, pdb3gao,
pdb3gaq, pdb3gar, pdb3gas, pdb3gat, pdb3gau, pdb3gav, pdb3gaw, pdb3gax, pdb3gay,
pdb3gaz, pdb3uq0, pdb3uq2, pdb3uq3, pdb3uq4, pdb3uq5, pdb3uq6, pdb3uq7, pdb3uq8,
pdb3uq9, pdb3uqa, pdb3uqb, pdb3uqc, pdb3uqd, pdb3uqe, pdb3uqf, pdb3uqg, pdb3uqh,
pdb3uqi, pdb3uqn, pdb3uqo, pdb3uqp, pdb3uqr, pdb3uqs, pdb3uqu, pdb3uqv, pdb3uqw,

```
pdb3uqx, pdb3uqy, pdb3uqz, pdb3zz1, pdb4a30, pdb4a31, pdb4a32, pdb4a33, pdb4a34,
pdb4a35, pdb4a36, pdb4a37, pdb4a38, pdb4a39, pdb4a3b, pdb4a3c, pdb4a3d, pdb4a3e,
pdb4a3f, pdb4a3g, pdb4a3h, pdb4a3i, pdb4a3j, pdb4a3k, pdb4a3l, pdb4a3m, pdb4a3n,
pdb4a3o, pdb4a3p, pdb4a3q, pdb4a3r, pdb4a3s, pdb4a3t, pdb4a3u, pdb4a3v, pdb4a3w,
pdb4a3x, pdb4a3y, pdb4a3z, pdb4dk0, pdb4dk1, pdb4dk2, pdb4dk3, pdb4dk4, pdb4dk5,
pdb4dk6, pdb4dk7, pdb4dk8, pdb4dk9, pdb4dka, pdb4dkb, pdb4dkc, pdb4dkd, pdb4dke,
pdb4dkf, pdb4dki, pdb4dkj, pdb4dkk, pdb4dkl, pdb4dkm, pdb4dkn, pdb4dko, pdb4dkp,
pdb4dkq, pdb4dkr, pdb4dks, pdb4dkt, pdb4dku, pdb4dkv, pdb4dkw, pdb4dkx, pdb4dky,
pdb4dkz, pdb4e50, pdb4e51, pdb4e52, pdb4e53, pdb4e54, pdb4e55, pdb4e56, pdb4e57,
pdb4e58, pdb4e59, pdb4e5a, pdb4e5b, pdb4e5c, pdb4e5d, pdb4e5e, pdb4e5f, pdb4e5g,
pdb4e5h, pdb4e5i, pdb4e5j, pdb4e5k, pdb4e5l, pdb4e5m, pdb4e5n, pdb4e5o, pdb4e5p,
pdb4e5q, pdb4e5r, pdb4e5s, pdb4e5t, pdb4e5u, pdb4e5v, pdb4e5w, pdb4e5x, pdb4e5y,
pdb4e5z, pdb4ef0, pdb4ef1, pdb4ef2, pdb4ef3, pdb4ef4, pdb4ef5, pdb4ef6, pdb4ef8,
pdb4ef9, pdb4efa, pdb4efb, pdb4efc, pdb4efd, pdb4efe, pdb4eff, pdb4efg, pdb4efh,
pdb4efi, pdb4efj, pdb4efk, pdb4efl, pdb4efm, pdb4efn, pdb4efo, pdb4efp, pdb4efq,
pdb4efr, pdb4efs, pdb4eft, pdb4efu, pdb4efv, pdb4efx, pdb4efz, pdb4fj0, pdb4fj1,
pdb4fj2, pdb4fj3, pdb4fj4, pdb4fj5, pdb4fj6, pdb4fj7, pdb4fj8, pdb4fj9, pdb4fjc,
pdb4fjg, pdb4fjh, pdb4fji, pdb4fjj, pdb4fjk, pdb4fjl, pdb4fjm, pdb4fjn, pdb4fjo,
pdb4fjp, pdb4fjq, pdb4fjr, pdb4fjs, pdb4fju, pdb4fjv, pdb4fjw, pdb4fjx, pdb4fjy,
pdb4fjz, pdb4fp1, pdb4fp2, pdb4fp3, pdb4fp4, pdb4fp5, pdb4fp6, pdb4fp7, pdb4fp8,
pdb4fp9, pdb4fpa, pdb4fpb, pdb4fpc, pdb4fpd, pdb4fpe, pdb4fpf, pdb4fpg, pdb4fph,
pdb4fpi, pdb4fpj, pdb4fpk, pdb4fpl, pdb4fpo, pdb4fpp, pdb4fpr, pdb4fps, pdb4fpt,
pdb4fpv, pdb4fpw, pdb4fpx, pdb4fpy, pdb4fpz, pdb4ga0, pdb4ga1, pdb4ga2, pdb4ga3,
pdb4ga4, pdb4ga5, pdb4ga6, pdb4ga7, pdb4ga8, pdb4ga9, pdb4gaa, pdb4gab, pdb4gac,
pdb4gad, pdb4gae, pdb4gaf, pdb4gag, pdb4gah, pdb4gai, pdb4gaj, pdb4gak, pdb4gal,
pdb4gam, pdb4gao, pdb4gap, pdb4gaq, pdb4gar, pdb4gas, pdb4gat, pdb4gau, pdb4gav,
pdb4gaw, pdb4gax, pdb4gay, pdb4gaz, pdb5a3h, pdb5gal, pdb5gat, pdb6a3h, pdb6gat,
pdb7a3h
```

1.4 Sample PDB-Hadoop job output

1.4.1 Dihedrals job output

A sample of the output from PDB-Hadoop during the computation of torsional (dihedral) angles on the PDB macro-molecular structure entries listed in section 1.3 above (discussed in chapter 5, section 5.5.1). NB: Only the first 20 records in the PDB is shown for two entries.

```
Extracted/writing file /tmp/pdb3gax.ent
pdb3gax.ent-0000000001 Phi,Psi,Omega,Chain,Residue
pdb3gax.ent-0000000002 1, 0.00, 164.35, 179.04, "A", "GLY12"
pdb3gax.ent-0000000003 2, -71.04, 145.47, -179.55, "A", "PRO13"
pdb3gax.ent-0000000004 3, -107.27, 154.17, 175.62, "A", "MET14"
pdb3gax.ent-0000000005 4, -58.21, 144.81, 175.34, "A", "ASP15"
pdb3gax.ent-0000000006 5, -141.64, 175.10, -178.81, "A", "ALA16"
pdb3gax.ent-0000000007 6, -143.17, 162.72, 177.07, "A", "SER17"
pdb3gax.ent-0000000008 7, -68.77, -13.42, 167.40, "A", "VAL18"
pdb3gax.ent-0000000009 8, -63.05, -22.24, -179.18, "A", "GLU19"
pdb3gax.ent-0000000010 9, -76.13, 128.76, -179.80, "A", "GLU20"
pdb3gax.ent-0000000011 10, -53.96, -43.56, 179.65, "A", "GLU21"
pdb3gax.ent-0000000012 11, -62.53, -44.40, 172.47, "A", "GLY22"
pdb3gax.ent-0000000013 12, -55.75, -47.94, 177.52, "A", "VAL23"
pdb3gax.ent-0000000014 13, -59.85, -41.82, 179.37, "A", "ARG24"
pdb3gax.ent-0000000015 14, -64.57, -44.26, 177.91, "A", "ARG25"
```

```
pdb3gax.ent-0000000016 15, -64.42, -39.67, 176.43, "A", "ALA26"
pdb3gax.ent-0000000017 16, -59.85, -49.39, -179.06, "A", "LEU27"
pdb3gax.ent-0000000018 17, -66.68, -41.04, 173.57, "A", "ASP28"
pdb3gax.ent-0000000019 18, -55.45, -52.34, -176.12, "A", "PHE29"
pdb3gax.ent-0000000020 19, -62.26, -45.43, 178.14, "A", "ALA30"
pdb3gax.ent-0000000021 20, -65.31, -41.39, 172.49, "A", "VAL31"
......
......
Extracted/writing file /tmp/pdb3zzs.ent
pdb3ga3.ent-0000000001 Phi,Psi,Omega,Chain,Residue
pdb3ga3.ent-0000000002 1, 0.00, -25.54, -177.36, "A", "ALA893"
pdb3ga3.ent-0000000003 2, -63.68, -21.97, 178.11, "A", "LYS894"
pdb3ga3.ent-0000000004 3, -103.02, 7.32, 178.37, "A", "HIS895"
pdb3ga3.ent-0000000005 4, -68.56, 160.12, 177.24, "A", "TYR896"
pdb3ga3.ent-0000000006 5, -92.42, 128.71, 179.37, "A", "LYS897"
pdb3ga3.ent-0000000007 6, -94.55, 50.91, -178.00, "A", "ASN898"
pdb3ga3.ent-0000000008 7, -133.32, 78.56, -179.84, "A", "ASN899"
pdb3ga3.ent-0000000009 8, -60.43, -21.70, 179.64, "A", "PRO900"
pdb3ga3.ent-0000000010 9, -63.02, -13.94, 179.82, "A", "SER901"
pdb3ga3.ent-0000000011 10, -70.68, -17.54, -176.86, "A", "LEU902"
pdb3ga3.ent-0000000012 11, -122.34, 157.51, 175.84, "A", "ILE903"
pdb3ga3.ent-0000000013 12, -132.36, 149.02, 179.17, "A", "THR904"
pdb3ga3.ent-0000000014 13, -111.26, 126.57, 178.44, "A", "PHE905"
pdb3ga3.ent-0000000015 14, -113.43, 144.65, 175.13, "A", "LEU906"
pdb3ga3.ent-0000000016 15, -58.98, 131.57, -177.90, "A", "CYS907"
pdb3ga3.ent-0000000017 16, -66.44, -22.86, -179.84, "A", "LYS908"
pdb3ga3.ent-0000000018 17, -89.35, -53.63, -176.44, "A", "ASN909"
pdb3ga3.ent-0000000019 18, -101.81, -4.60, 178.96, "A", "CYS910"
pdb3ga3.ent-0000000020 19, 69.58, 7.36, 179.63, "A", "SER911"
pdb3ga3.ent-0000000021 20, -68.24, 147.11, 177.33, "A", "VAL912"
......
......
```

1.4.2 Docking job output

Below is a sample of the output from PDB-Hadoop during the docking of a small oligo-peptide (discussed in chapter 5, section 5.5.2) against the PDB macro-molecular entries listed in section 1.3 above. The output employs the *post-processing* step of PDB-Hadoop to extract docking scores from Vina AutoDock and summarise them in order of best (lowest energy) docking score.

```
Extracted/writing file /tmp/pdb1a3q.ent
Initiating post-processing...
pdb1a3q.ent-0000000001     1         -4.6      0.000      0.000
pdb1a3q.ent-0000000002     2         -4.4     22.399     23.769
pdb1a3q.ent-0000000003     3         -4.2     22.208     22.970
pdb1a3q.ent-0000000004     4         -4.2     19.226     21.204
pdb1a3q.ent-0000000005     5         -4.1     34.622     36.402
pdb1a3q.ent-0000000006     6         -4.0     20.313     22.641
pdb1a3q.ent-0000000007     7         -4.0     34.348     35.354
pdb1a3q.ent-0000000008     8         -4.0     27.283     29.148
pdb1a3q.ent-0000000009     9         -3.9     26.239     27.588
Extracted/writing file /tmp/pdb2dkr.ent
Initiating post-processing...
```

```
pdb2dkr.ent-0000000001     1         -5.0      0.000      0.000
pdb2dkr.ent-0000000002     2         -4.7      3.496      5.931
pdb2dkr.ent-0000000003     3         -4.6      3.759      4.530
pdb2dkr.ent-0000000004     4         -4.6      5.178      6.929
pdb2dkr.ent-0000000005     5         -4.4     24.758     26.165
pdb2dkr.ent-0000000006     6         -4.3      2.661      3.299
pdb2dkr.ent-0000000007     7         -4.2     21.788     22.757
pdb2dkr.ent-0000000008     8         -4.0     17.432     19.035
pdb2dkr.ent-0000000009     9         -4.0     14.814     15.540
......
......
```

Appendix 2

Transcriptomics analysis (Chapter 6)

2.1 Preparation for MapReduce on Apache Spark

Prior to running the analyses, as we are examining *intra-exon* motif correlations (correlations of *k-mer* motifs within the same exon), the genome annotation GTF file must be filtered to only include *exon* feature records in the tuples file G, which serves as a reference input to the Spark Job. Furthermore, as the *quality score* field of the SAM alignments file can contain a comma and this field is unused in the analyses we remove all the comma characters using the *tr* Linux command to produce the cleaned SAM reads file S, which is input to the Spark Job.

The Apache Spark cluster used utilises the YARN scheduler and is comprised of a master node which has an Intel E5-2620 hexa-core CPU @ 2.10 GHz and 32 GB of RAM, and 5 slave nodes, each node has an Intel Xeon E3-1220v3 4-core CPU @ 3.1GHz and 32 GB RAM per node. As the master node is configured solely to schedule jobs and not run them directly, and each slave compute node has a 4-core CPU, a total of 20 CPU cores are available for computation across all of the compute nodes of the cluster, excluding the master. In order to optimise the running of the analyses for each dataset on Spark we explicitly set the number of YARN executors and cores for the job, which ideally should be a slightly less than a multiple of the number of nodes and total CPU cores/node respectively, to allow for some resources to be left available for the OS. We therefore set the number of *executors* at 5 as there are a total of six nodes, but the master does not execute jobs directly, and the number of *cores* per executor at 3, giving a total of 15 cores available for computation across the cluster. Because there are 4 cores/node this leaves 1 core/node and 4 GB/node available for the OS and therefore 3 cores/node and 28 GB/node is available for running Spark Jobs.

2.2 Results for testing of synthetic transcriptome reads

Pearson correlation outliers - Synthetic reads			
Lowest 10 Pearson-correlation outliers and their motifs			
R(10 bp)	R(50 bp)	R(100 bp)	R(200 bp)
TCAA=1.0000	GCCG=1.0000	AAAG=1.0000	GTTA=1.0000
CTGG=1.0000	GAGC=1.0000	ACCA=1.0000	TGGC=1.0000
GTAA=1.0000	TCGC=1.0000	AAGT=1.0000	TGCT=1.0000
CATC=1.0000	GTTA=1.0000	TTTA=1.0000	TTCG=1.0000
TCCA=1.0000	CATC=1.0000	GCCG=1.0000	CCGG=1.0000
ATTT=1.0000	TACA=1.0000	CCGT=1.0000	ACTA=1.0000
AAGC=1.0000	TTTA=1.0000	GAGA=1.0000	GCCA=1.0000
CAGA=1.0000	CCGG=1.0000	AACG=1.0000	TAAA=1.0000
CCGC=1.0000	GCTC=1.0000	GAAC=1.0000	ATAG=1.0000
GGAC=1.0000	CCTT=1.0000	TAAA=1.0000	GTAA=1.0000
Highest 10 Pearson-correlation outliers and their motifs			
R(10 bp)	R(50 bp)	R(100 bp)	R(200 bp)
GAGG=1.0000	CCTT=1.0000	TCAA=1.0000	TATG=1.0000
AAAG=1.0000	CTGC=1.0000	TCAT=1.0000	GACT=1.0000
GGCA=1.0000	GGTT=1.0000	TATG=1.0000	GAGG=1.0000
AGCC=1.0000	GGCC=1.0000	CTGC=1.0000	AAAG=1.0000
AGTA=1.0000	ATCC=1.0000	ACCT=1.0000	GAGT=1.0000
CGGA=1.0000	ATCG=1.0000	TACG=1.0000	CACA=1.0000
GTAT=1.0000	AGCC=1.0000	CGAT=1.0000	CAAC=1.0000
CGTA=1.0000	CCTG=1.0000	TCCT=1.0000	TACC=1.0000
TAAG=1.0000	CTTT=1.0000	GGTT=1.0000	AGCC=1.0000
CACC=1.0000	CTCT=1.0000	GAGG=1.0000	AGAA=1.0000

Table 2.1: Correlation in synthetically generated transcriptomic reads. Table summarises Pearson correlation co-efficient outliers (top ten and lowest ten) for different *4-mer* motif occurrences at 10, 50, 100 and 200 bp.

2.3 Wild-type *D. melanogaster* results

Motif spacing: **10bp**								
Exon GC%	**30-40%**		**40-50%**		**50-60%**		**60-70%**	
Motif GC%	50	0	50	0	50	0	50	0
#Correlations	16	96	16	96	16	96	8	96
p(t-test)	$4.83\text{x}10^{-4}(1.54\text{x}10^{-3})$*		$9.91\text{x}10^{-1}(9.91\text{x}10^{-1})$		$6.56\text{x}10^{-1}(7.50\text{x}10^{-1})$		$3.50\text{x}10^{-1}(4.38\text{x}10^{-1})$	
p(Wilcoxon)	$8.79\text{x}10^{-2}(1.41\text{x}10^{-1})$		$1.96\text{x}10^{-1}(2.61\text{x}10^{-1})$		$4.69\text{x}10^{-1}(5.36\text{x}10^{-1})$		1.00(1.00)	
Exon GC%	**30-40%**		**40-50%**		**50-60%**		**60-70%**	
Motif GC%	50	25	50	25	50	25	50	25
#Correlations	64	96	64	96	64	96	54	96
p(t-test)	$7.66\text{x}10^{-3}(1.53\text{x}10^{-2})$*		$8.53\text{x}10^{-1}(9.10\text{x}10^{-1})$		$3.31\text{x}10^{-1}(4.38\text{x}10^{-1})$		$4.81\text{x}10^{-2}(8.55\text{x}10^{-2})$	
p(Wilcoxon)	$5.40\text{x}10^{-3}(1.73\text{x}10^{-2})$*		$9.52\text{x}10^{-1}(1.00)$		$1.83\text{x}10^{-1}(2.61\text{x}10^{-1})$		$8.58\text{x}10^{-2}(1.41\text{x}10^{-1})$	
Exon GC%	**30-40%**		**40-50%**		**50-60%**		**60-70%**	
Motif GC%	50	75	50	75	50	75	50	75
#Correlations	64	96	64	96	64	96	64	96
p(t-test)	$1.40\text{x}10^{-1}(2.25\text{x}10^{-1})$		$3.55\text{x}10^{-1}(4.38\text{x}10^{-1})$		$6.26\text{x}10^{-3}(1.43\text{x}10^{-2})$*		$9.88\text{x}10^{-5}(3.95\text{x}10^{-4})$*	
p(Wilcoxon)	$2.30\text{x}10^{-2}(4.60\text{x}10^{-2})$*		$4.11\text{x}10^{-1}(5.06\text{x}10^{-1})$		$1.00\text{x}10^{-2}(2.68\text{x}10^{-2})$*		$8.07\text{x}10^{-4}(1.28\text{x}10^{-2})$*	
Exon GC%	**30-40%**		**40-50%**		**50-60%**		**60-70%**	
Motif GC%	50	100	50	100	50	100	50	100
#Correlations	16	96	16	96	16	96	16	96
p(t-test)	$1.08\text{x}10^{-3}(2.89\text{x}10^{-3})$*		$4.82\text{x}10^{-6}(2.57\text{x}10^{-5})$*		$2.28\text{x}10^{-6}(1.82\text{x}10^{-5})$*		$3.45\text{x}10^{-8}(5.52\text{x}10^{-7})$*	
p(Wilcoxon)	$1.31\text{x}10^{-2}(2.99\text{x}10^{-2})$*		$2.71\text{x}10^{-3}(1.28\text{x}10^{-2})$*		$1.92\text{x}10^{-3}(1.28\text{x}10^{-2})$*		$3.20\text{x}10^{-3}(1.28\text{x}10^{-2})$*	

Table 2.2: T-test and Wilcoxon-test comparisons of Pearson correlations for motif-pairs at 10bp spacing for varying motif GC and mean exon GC content in Wild-type *D. melanogaster*. FDR corrected p-values in parenthesis, using a False positive rate of 5% ($\alpha = 0.05$). * suggests rejection of the null hypothesis.

Motif spacing: **50bp**								
Exon GC%	**30-40%**		**40-50%**		**50-60%**		**60-70%**	
Motif GC%	50	0	50	0	50	0	50	0
#Correlations	16	96	16	96	16	96	4	96
p(t-test)	$2.87\text{x}10^{-2}(7.07\text{x}10^{-2})$		$4.94\text{x}10^{-1}(6.32\text{x}10^{-1})$		$9.91\text{x}10^{-1}(9.91\text{x}10^{-1})$		$5.58\text{x}10^{-1}(6.87\text{x}10^{-1})$	
p(Wilcoxon)	$5.23\text{x}10^{-3}(2.47\text{x}10^{-2})$*		$4.38\text{x}10^{-1}(5.84\text{x}10^{-1})$		$5.35\text{x}10^{-1}(6.58\text{x}10^{-1})$		1.00(1.00)	
Exon GC%	**30-40%**		**40-50%**		**50-60%**		**60-70%**	
Motif GC%	50	25	50	25	50	25	50	25
#Correlations	64	96	64	96	64	96	46	96
p(t-test)	$3.89\text{x}10^{-1}(5.42\text{x}10^{-1})$		$4.87\text{x}10^{-1}(6.32\text{x}10^{-1})$		$8.69\text{x}10^{-1}(9.31\text{x}10^{-1})$		$1.63\text{x}10^{-1}(2.75\text{x}10^{-1})$	
p(Wilcoxon)	$1.58\text{x}10^{-1}(2.81\text{x}10^{-1})$		$3.29\text{x}10^{-1}(4.78\text{x}10^{-1})$		$8.94\text{x}10^{-1}(9.86\text{x}10^{-1})$		$7.97\text{x}10^{-1}(9.11\text{x}10^{-1})$	
Exon GC%	**30-40%**		**40-50%**		**50-60%**		**60-70%**	
Motif GC%	50	75	50	75	50	75	50	75
#Correlations	61	96	64	96	64	96	64	96
p(t-test)	$8.73\text{x}10^{-1}(9.31\text{x}10^{-1})$		$1.15\text{x}10^{-1}(2.17\text{x}10^{-1})$		$7.15\text{x}10^{-2}(1.51\text{x}10^{-1})$		$7.53\text{x}10^{-2}(1.51\text{x}10^{-1})$	
p(Wilcoxon)	$7.82\text{x}10^{-1}(9.11\text{x}10^{-1})$		$5.49\text{x}10^{-2}(1.17\text{x}10^{-1})$		$2.04\text{x}10^{-1}(3.11\text{x}10^{-1})$		$4.30\text{x}10^{-3}(2.47\text{x}10^{-2})$*	
Exon GC%	**30-40%**		**40-50%**		**50-60%**		**60-70%**	
Motif GC%	50	100	50	100	50	100	50	100
#Correlations	16	96	16	96	16	96	16	96
p(t-test)	$5.69\text{x}10^{-3}(2.00\text{x}10^{-2})$*		$1.06\text{x}10^{-2}(2.82\text{x}10^{-2})$*		$1.36\text{x}10^{-3}(5.42\text{x}10^{-3})$*		$7.23\text{x}10^{-5}(5.78\text{x}10^{-4})$*	
p(Wilcoxon)	$9.73\text{x}10^{-3}(3.21\text{x}10^{-2})$*		$1.74\text{x}10^{-2}(4.63\text{x}10^{-2})$*		$8.36\text{x}10^{-3}(3.21\text{x}10^{-2})$*		$2.00\text{x}10^{-2}(4.92\text{x}10^{-2})$*	

Table 2.3: T-test and Wilcoxon-test comparisons of Pearson correlations for motif-pairs at 50bp spacing for varying motif GC and mean exon GC content in Wild-type *D. melanogaster*. FDR corrected p-values in parenthesis, using a False positive rate of 5% ($\alpha = 0.05$). * suggests rejection of the null hypothesis.

Motif spacing: **100bp**								
Exon GC%	**30-40%**		**40-50%**		**50-60%**		**60-70%**	
Motif GC%	50	0	50	0	50	0	50	0
#Correlations	16	96	16	96	16	96	3	96
p(t-test)	$1.31x10^{-2}(3.14x10^{-2})$*		$2.03x10^{-2}(4.64x10^{-2})$*		$4.54x10^{-1}(5.73x10^{-1})$		$1.06x10^{-4}(5.66x10^{-4})$*	
p(Wilcoxon)	$8.79x10^{-2}(1.62x10^{-1})$		$2.78x10^{-1}(3.92x10^{-1})$		$6.05x10^{-1}(6.92x10^{-1})$		$1.09x10^{-1}(1.87x10^{-1})$	
Exon GC%	**30-40%**		**40-50%**		**50-60%**		**60-70%**	
Motif GC%	50	25	50	25	50	25	50	25
#Correlations	64	96	64	96	64	96	52	96
p(t-test)	$1.31x10^{-1}(2.17x10^{-1})$		$4.58x10^{-2}(9.16x10^{-2})$		$4.51x10^{-2}(9.16x10^{-2})$		$5.57x10^{-1}(6.38x10^{-1})$	
p(Wilcoxon)	$8.09x10^{-2}(1.62x10^{-1})$		$1.73x10^{-2}(4.63x10^{-2})$*		$1.06x10^{-1}(1.87x10^{-1})$		$4.39x10^{-1}(5.40x10^{-1})$	
Exon GC%	**30-40%**		**40-50%**		**50-60%**		**60-70%**	
Motif GC%	50	75	50	75	50	75	50	75
#Correlations	64	96	64	96	64	96	64	96
p(t-test)	$3.23x10^{-1}(4.68x10^{-1})$		$6.12x10^{-3}(1.77x10^{-2})$*		$3.11x10^{-1}(4.67x10^{-1})$		$1.28x10^{-3}(4.65x10^{-3})$*	
p(Wilcoxon)	$1.45x10^{-1}(2.40x10^{-1})$		$3.46x10^{-2}(7.90x10^{-2})$		$3.99x10^{-1}(5.33x10^{-1})$		$3.26x10^{-3}(2.23x10^{-2})$*	
Exon GC%	**30-40%**		**40-50%**		**50-60%**		**60-70%**	
Motif GC%	50	100	50	100	50	100	50	100
#Correlations	16	96	16	96	16	96	16	96
p(t-test)	$5.91x10^{-4}(2.58x10^{-3})$*		$2.93x10^{-9}(7.03x10^{-8})$*		$1.84x10^{-6}(2.19x10^{-5})$*		4.67E-11$(2.24x10^{-9})$*	
p(Wilcoxon)	$1.51x10^{-2}(4.53x10^{-2})$*		$1.12x10^{-3}(1.80x10^{-2})$*		$1.31x10^{-2}(4.18x10^{-2})$*		$7.76x10^{-4}(1.80x10^{-2})$*	

Table 2.4: T-test and Wilcoxon-test comparisons of Pearson correlations for motif-pairs at 100bp spacing for varying motif GC and mean exon GC content in Wild-type *D. melanogaster*. FDR corrected p-values in parenthesis, using a False positive rate of 5% ($\alpha = 0.05$). * suggests rejection of the null hypothesis.

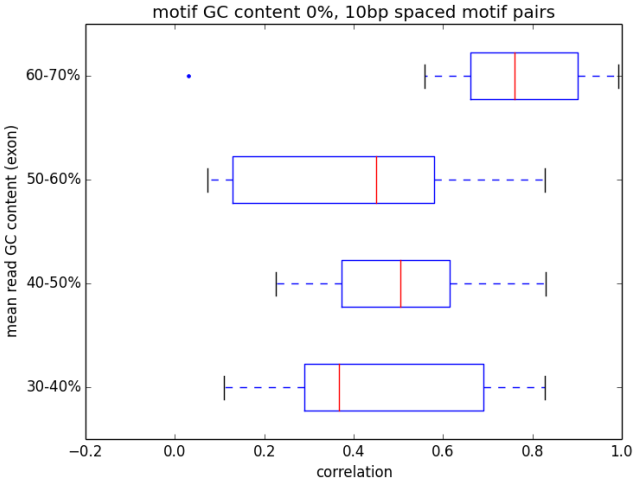

(a) Motif GC content of 0%

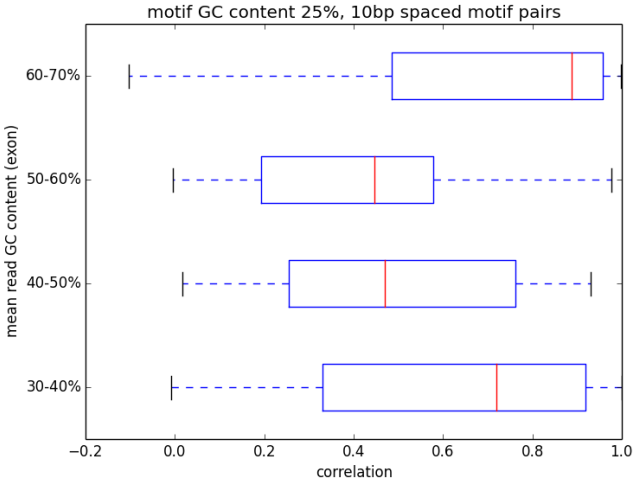

(b) Motif GC content of 25%

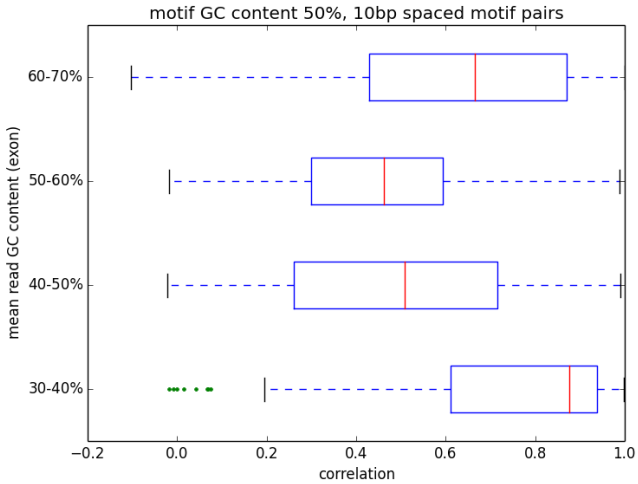

(c) Motif GC content of 50%

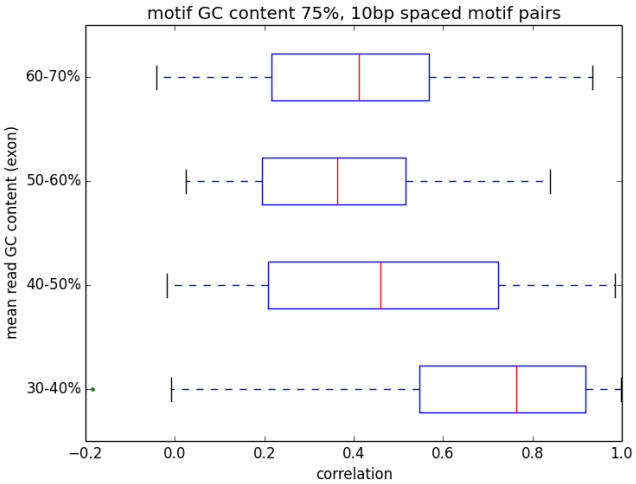

(d) Motif GC content of 75%

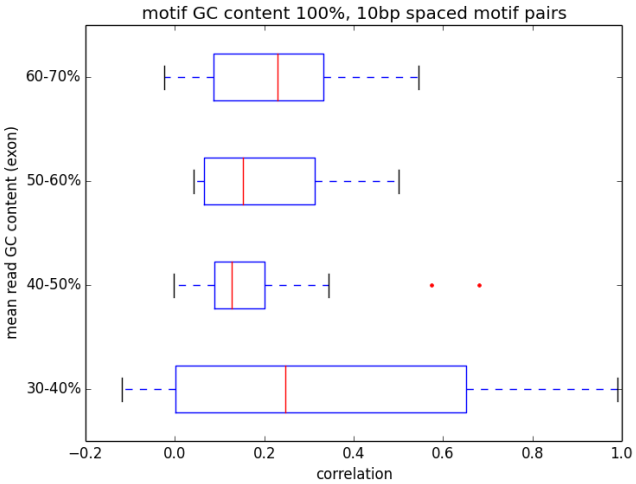

(e) Motif GC content of 100%

Figure 2.1: Box and whisker plots of motif-pair correlations at a distance of 10bp for Wild-type *D. melanogaster*

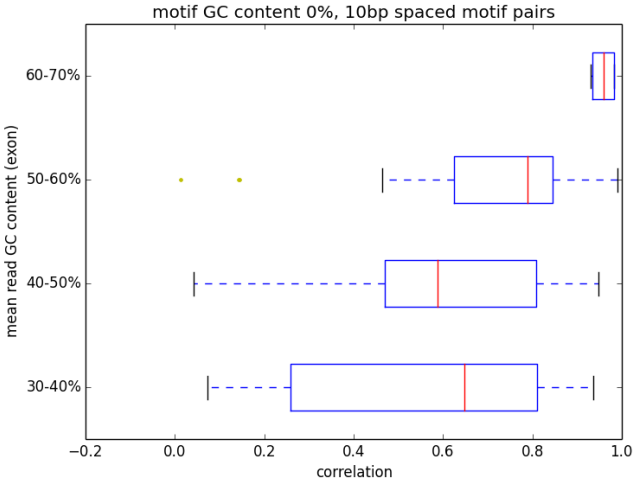

(a) Motif GC content of 0%

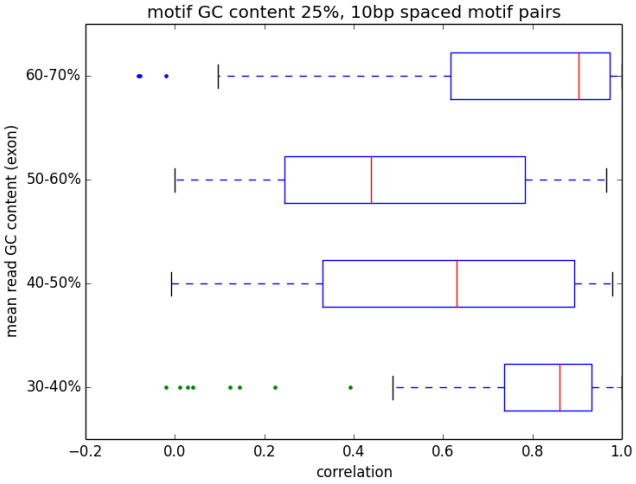

(b) Motif GC content of 25%

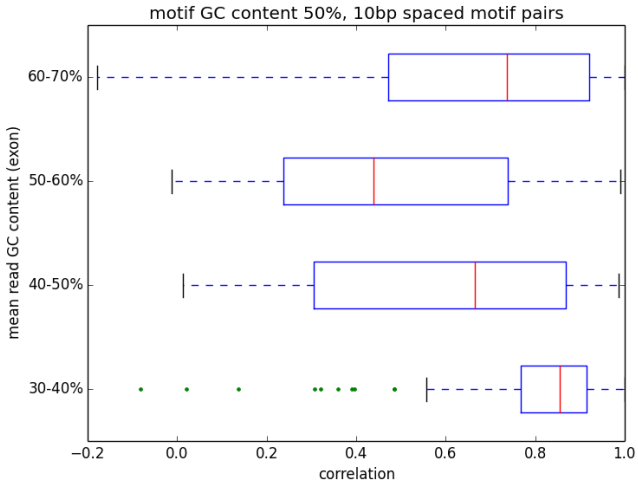

(c) Motif GC content of 50%

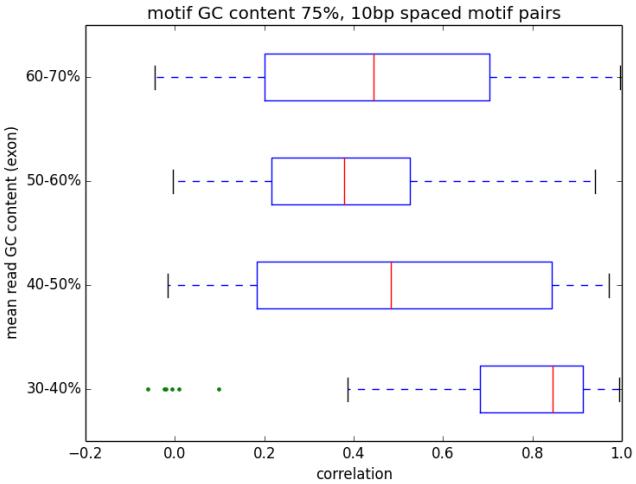

(d) Motif GC content of 75%

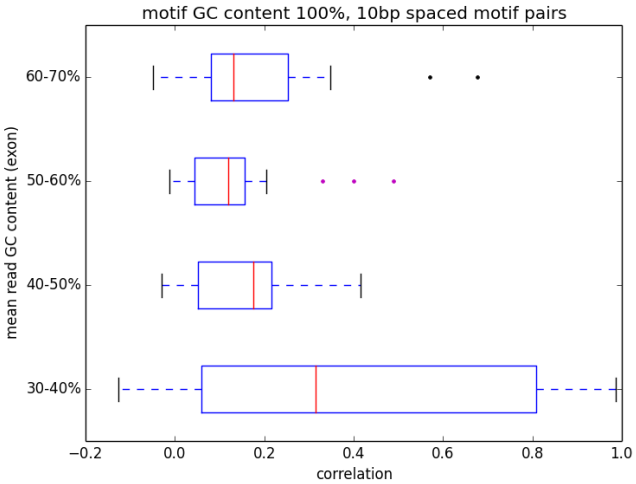

(e) Motif GC content of 100%

Figure 2.2: Box and whisker plots of motif pair correlations at a distance of 10bp for Wild-type *D. melanogaster* (Excluding hexamer regions)

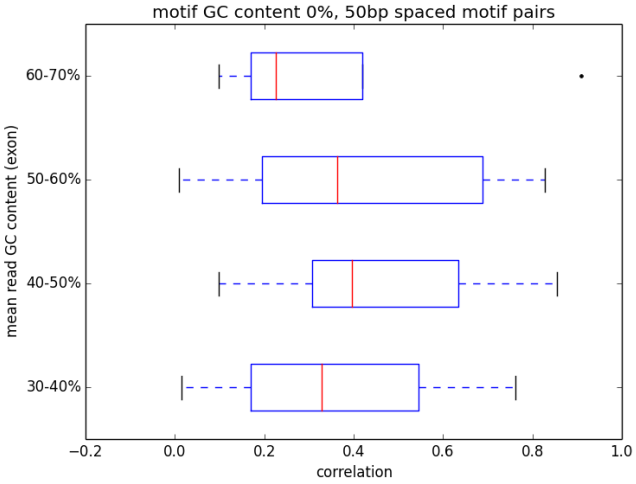

(a) Motif GC content of 0%

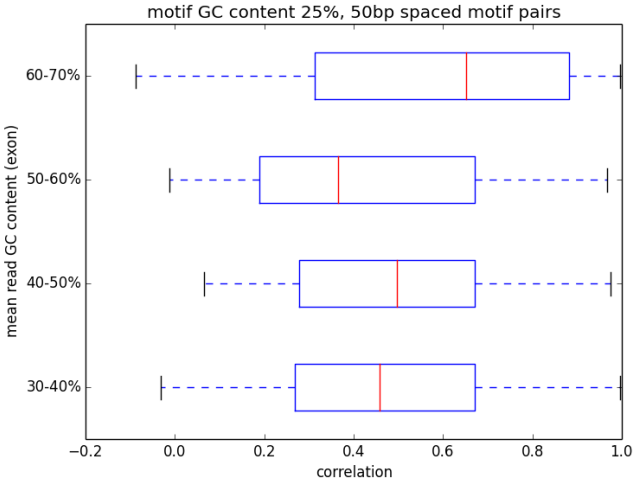

(b) Motif GC content of 25%

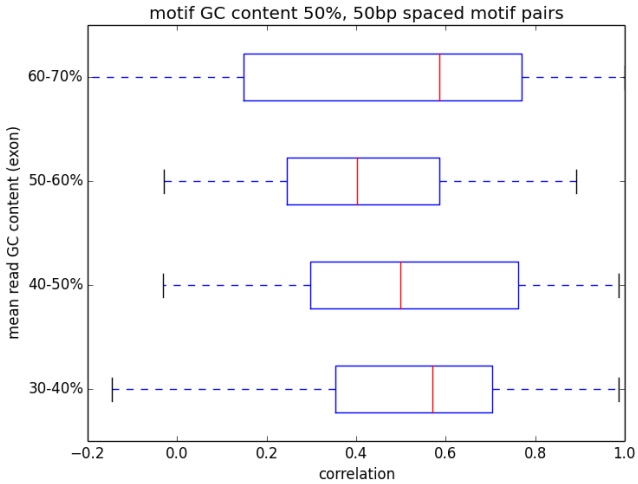

(c) Motif GC content of 50%

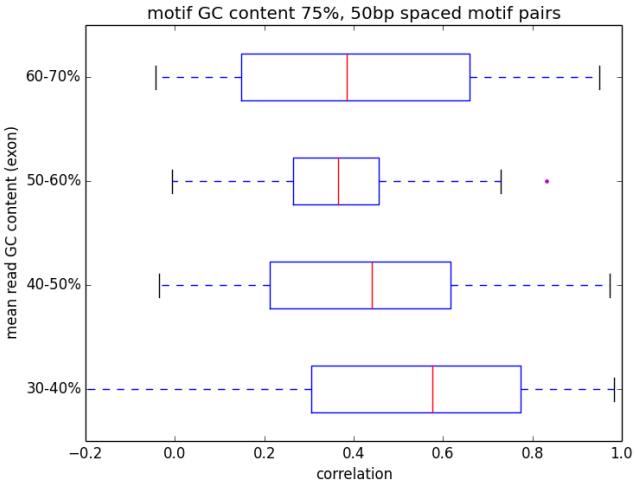

(d) Motif GC content of 75%

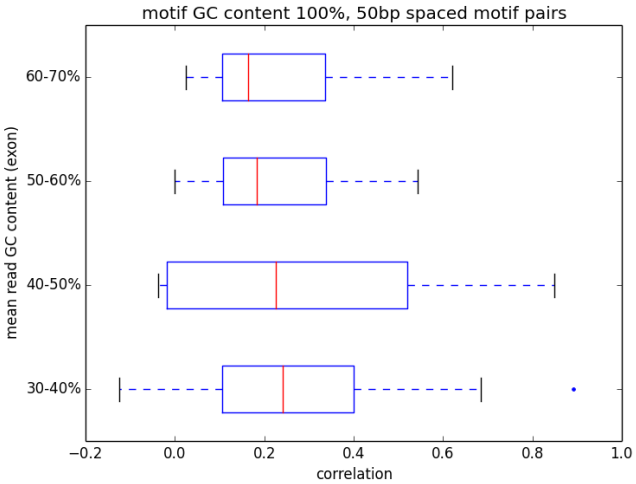

(e) Motif GC content of 100%

Figure 2.3: Box and whisker plots of motif-pair correlations at a distance of 50bp for Wild-type *D. melanogaster*

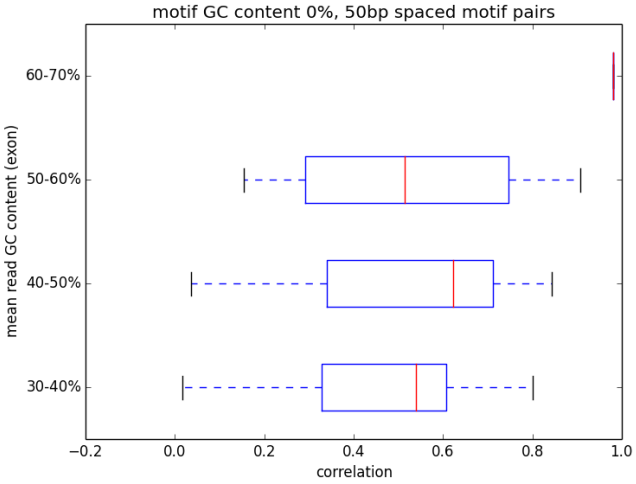

(a) Motif GC content of 0%

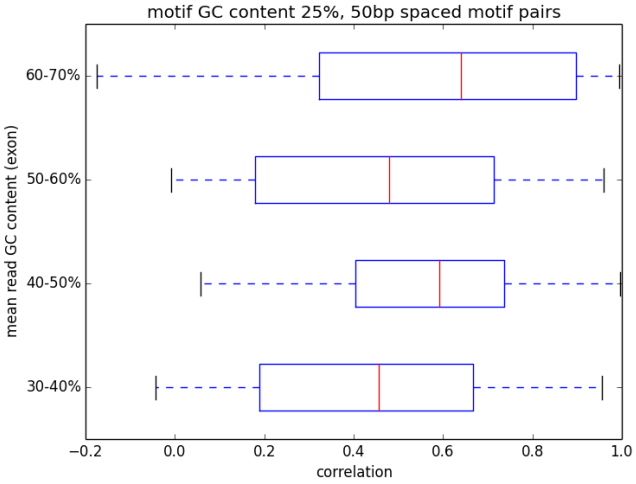

(b) Motif GC content of 25%

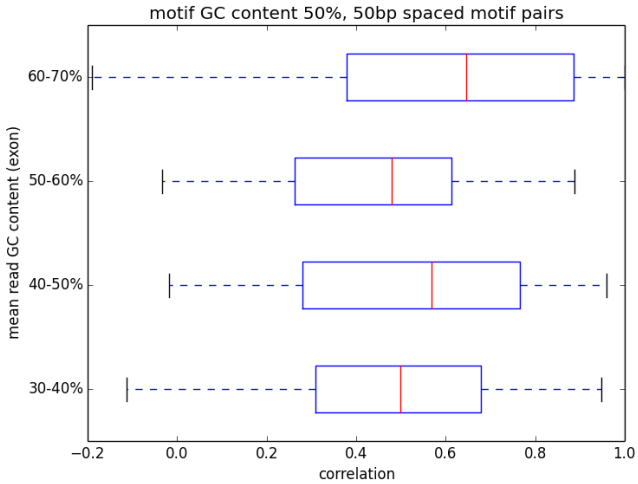

(c) Motif GC content of 50%

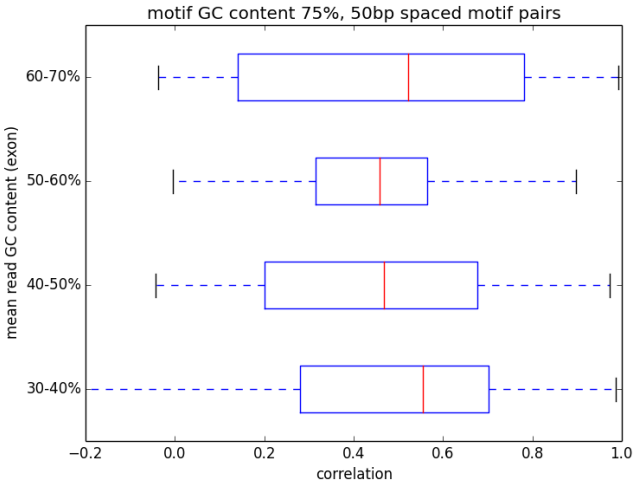

(d) Motif GC content of 75%

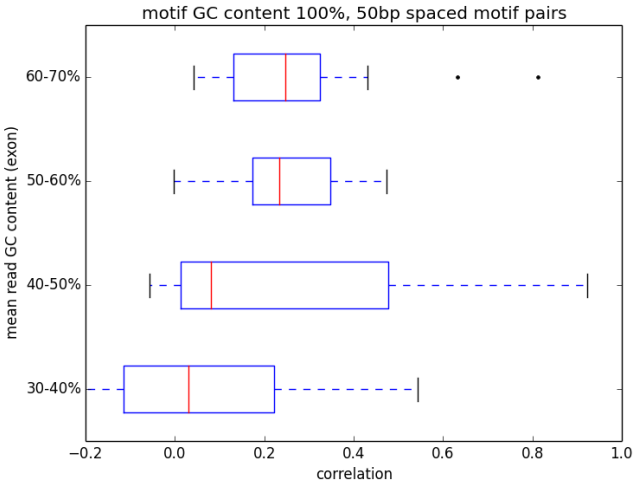

(e) Motif GC content of 100%

Figure 2.4: Box and whisker plots of motif pair correlations at a distance of 50bp for Wild-type *D. melanogaster* (Excluding hexamer regions)

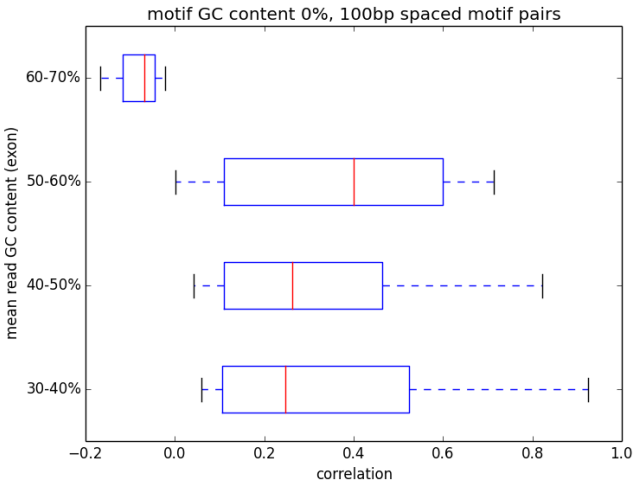

(a) Motif GC content of 0%

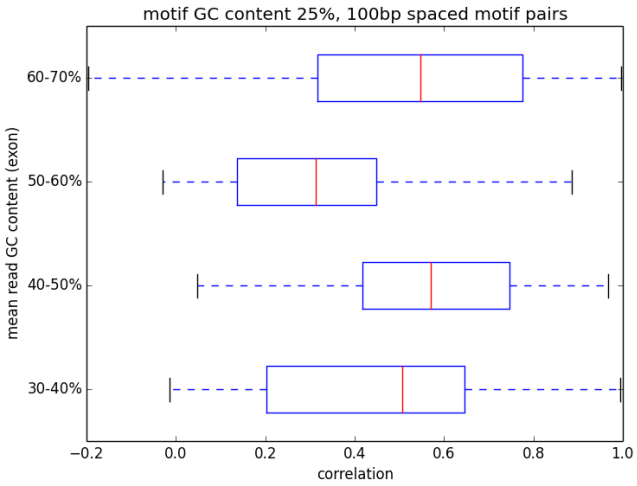

(b) Motif GC content of 25%

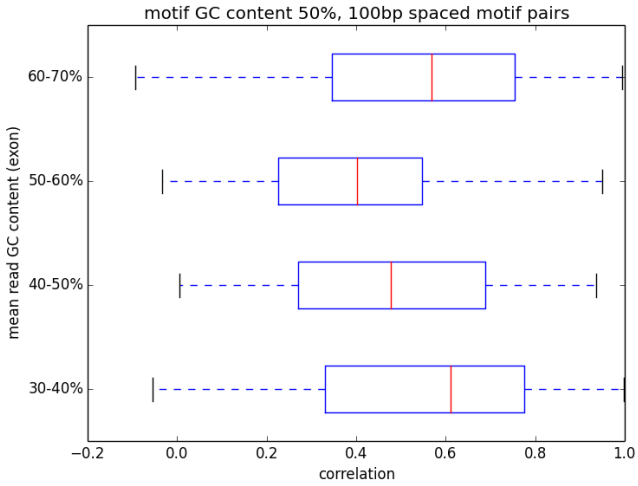

(c) Motif GC content of 50%

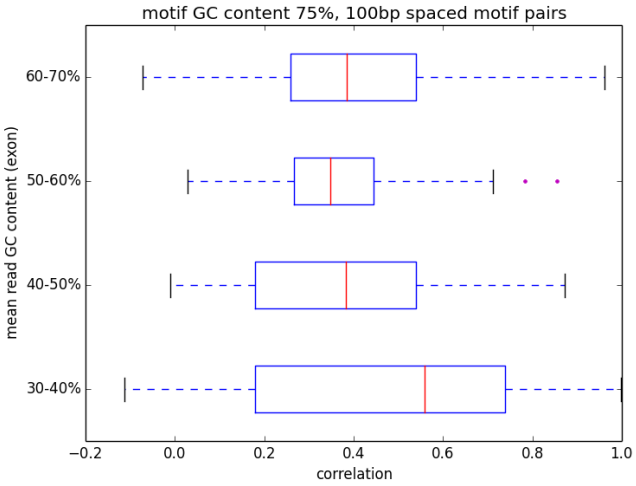

(d) Motif GC content of 75%

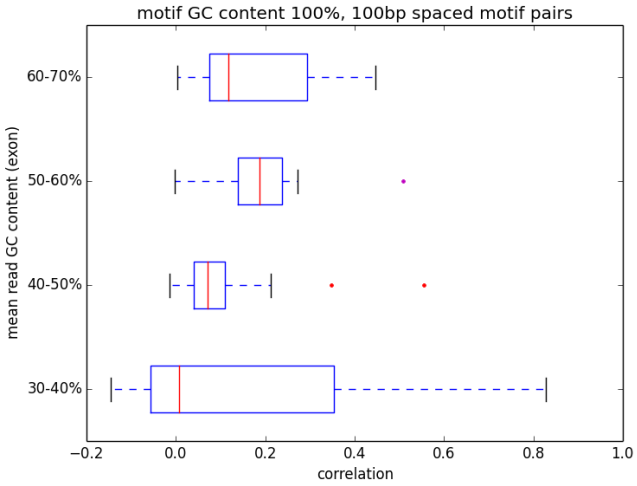

(e) Motif GC content of 100%

Figure 2.5: Box and whisker plots of motif-pair correlations at a distance of 100bp for Wild-type *D. melanogaster*.

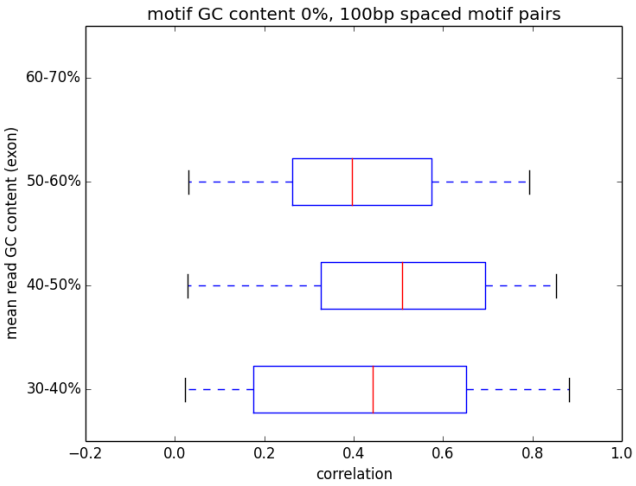

(a) Motif GC content of 0%

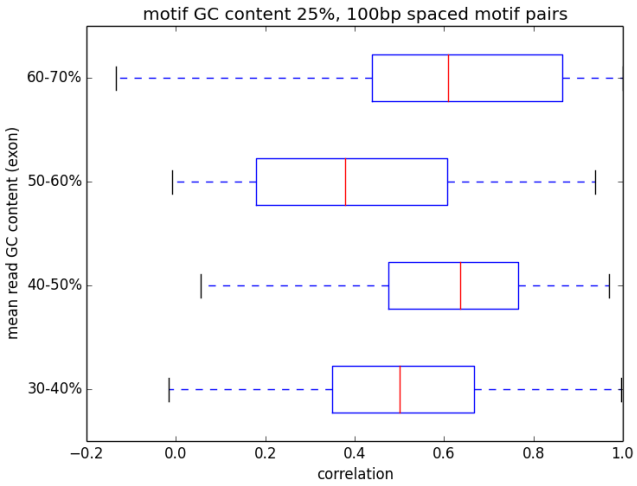

(b) Motif GC content of 25%

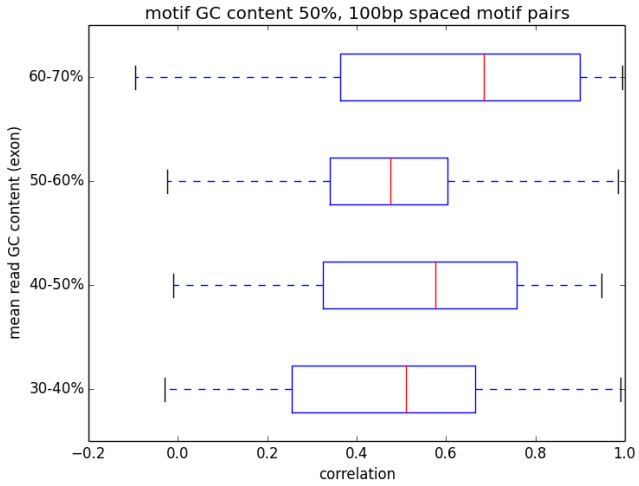

(c) Motif GC content of 50%

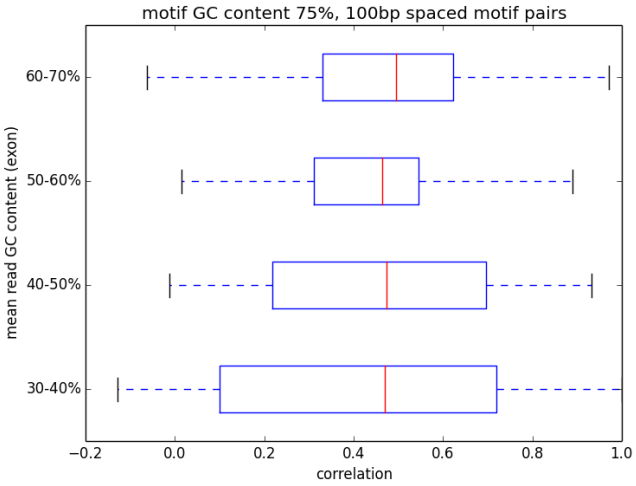

(d) Motif GC content of 75%

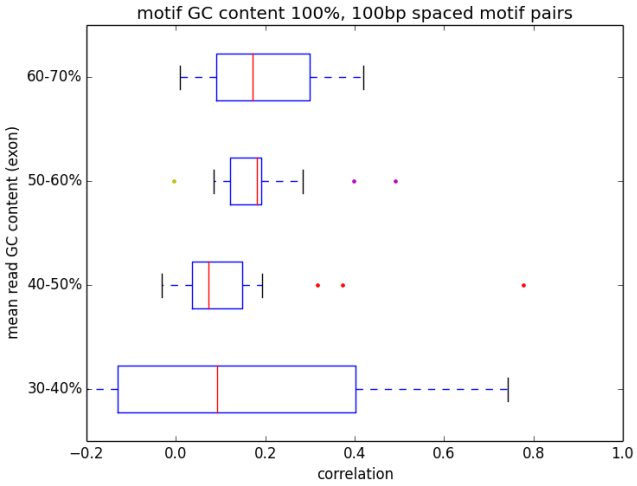

(e) Motif GC content of 100%

Figure 2.6: Box and whisker plots of motif pair correlations at a distance of 100bp for Wild-type *D. melanogaster* (Excluding hexamer regions)

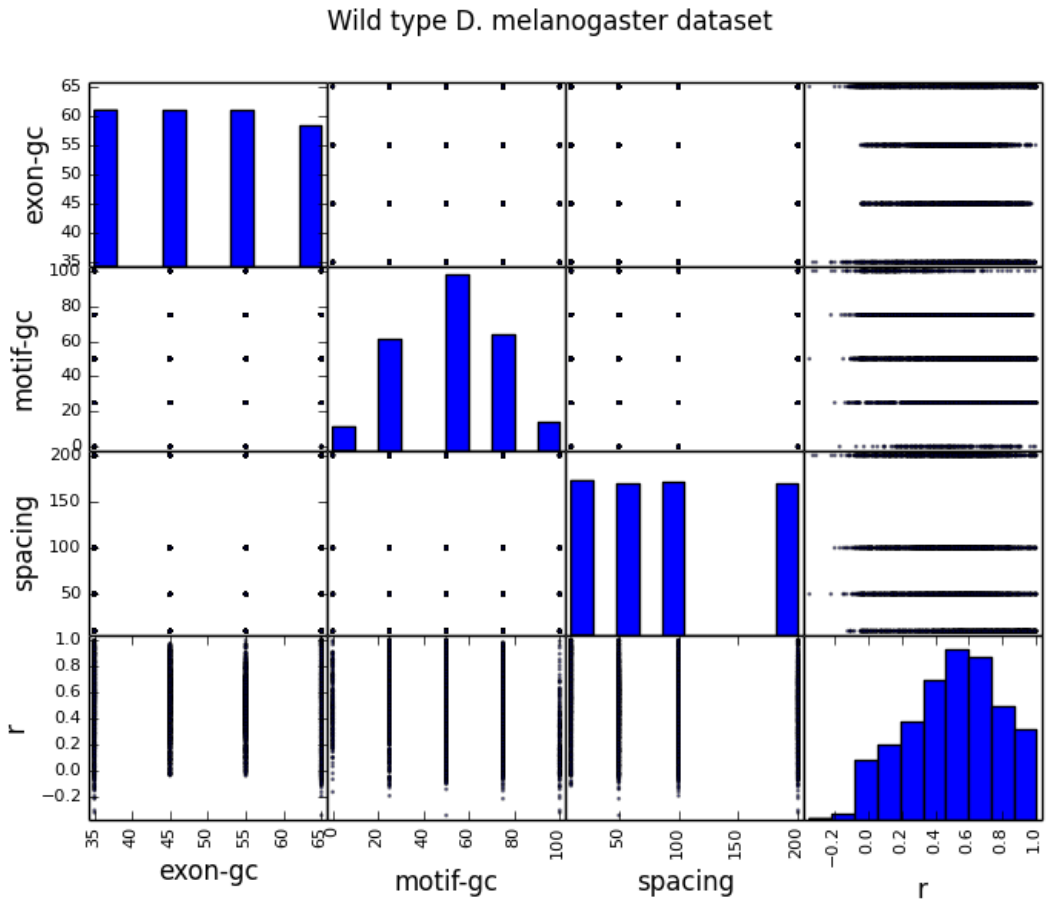

Figure 2.7: Scatter-matrix plot of correlation as a function of *4-mer* motif and exon GC content in wild type *D. melanogaster*.

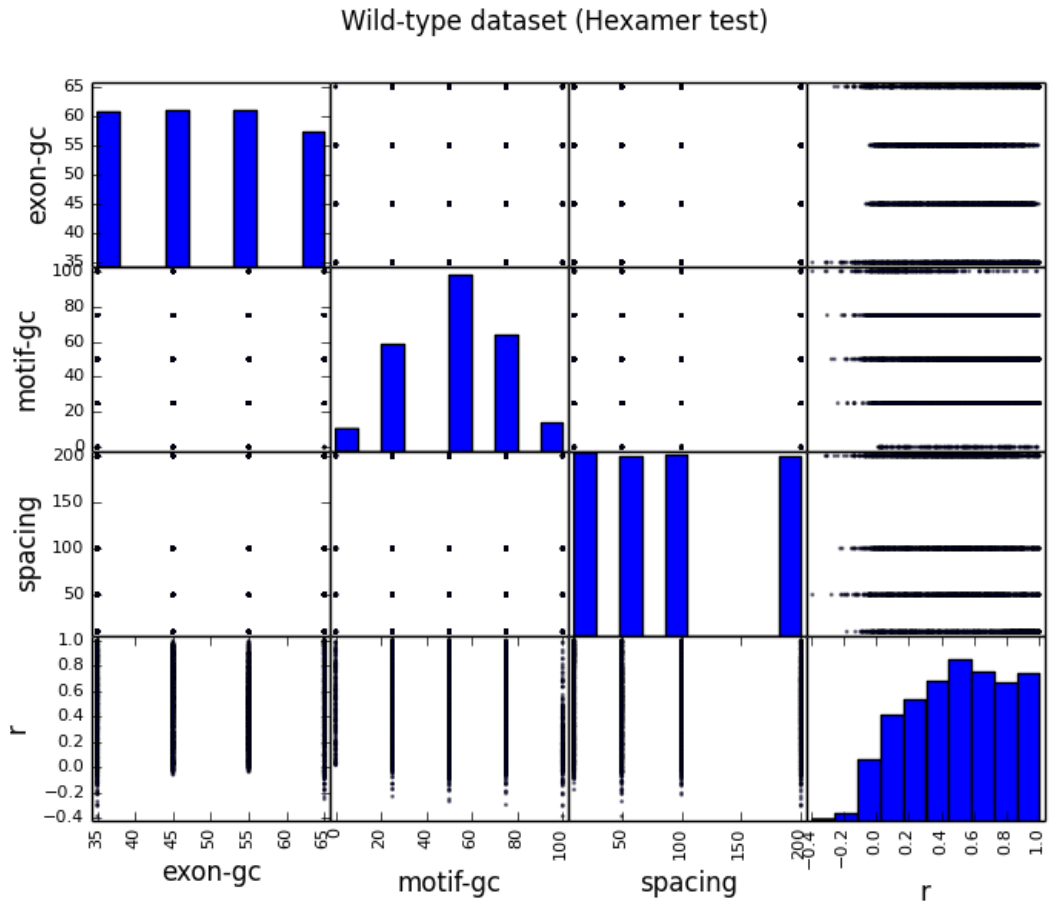

Figure 2.8: Scatter-matrix plot of correlation as a function of *4-mer* motif and exon GC content in wild type *D. melanogaster*. Random hexamer priming region has been excluded.

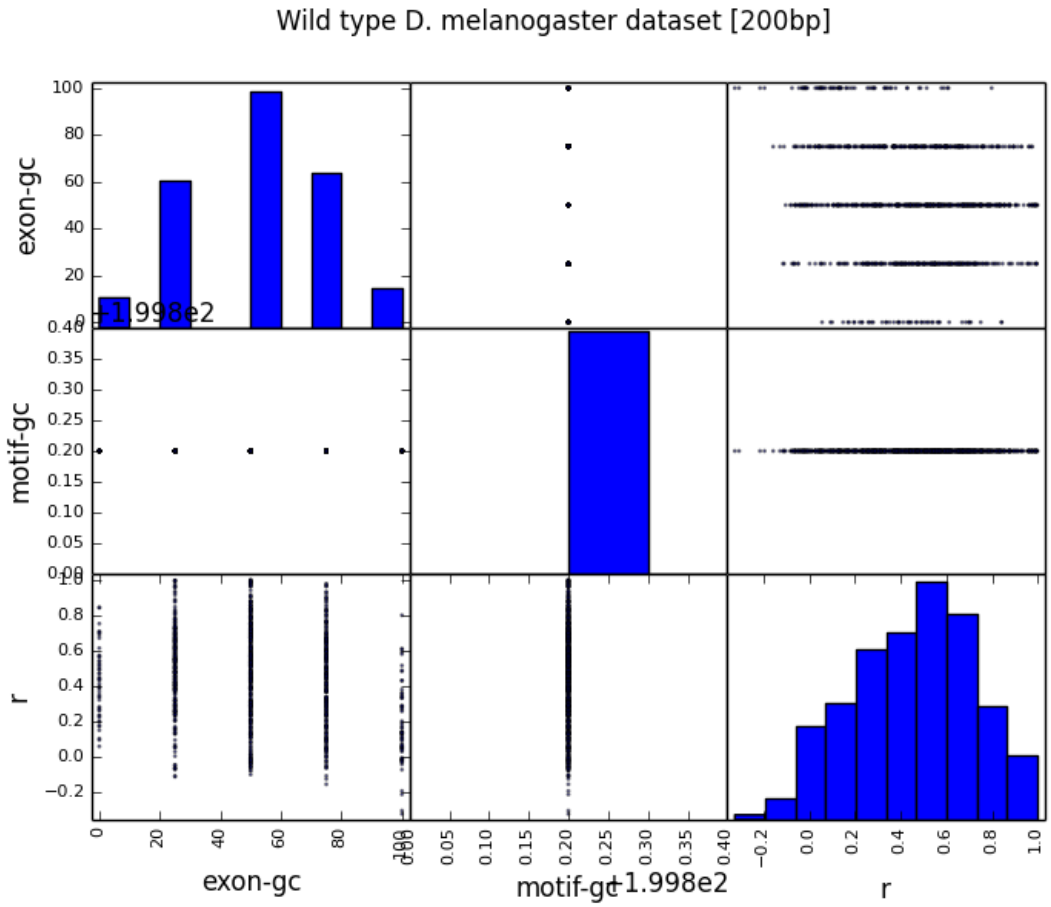

Figure 2.9: Scatter-matrix plot of correlation as a function of *4-mer* motif and exon GC content in wild type *D. melanogaster* at a motif-pair spacing of 200bp.

2.4 Mutant-r2-type *D. melanogaster* results

Motif spacing: **10bp**								
Exon GC%	**30-40%**		**40-50%**		**50-60%**		**60-70%**	
Motif GC%	50	0	50	0	50	0	50	0
#Correlations	16	96	16	96	16	96	16	96
p(t-test)	$2.15\text{x}10^{-3}(1.15\text{x}10^{-2})$*		$3.94\text{x}10^{-1}(5.25\text{x}10^{-1})$		$2.02\text{x}10^{-1}(3.90\text{x}10^{-1})$		$9.55\text{x}10^{-1}(9.55\text{x}10^{-1})$	
p(Wilcoxon)	$6.05\text{x}10^{-1}(6.45\text{x}10^{-1})$		$5.69\text{x}10^{-1}(6.45\text{x}10^{-1})$		$3.26\text{x}10^{-1}(4.74\text{x}10^{-1})$		$1.48\text{x}10^{-1}(3.38\text{x}10^{-1})$	
Exon GC%	**30-40%**		**40-50%**		**50-60%**		**60-70%**	
Motif GC%	50	25	50	25	50	25	50	25
#Correlations	64	96	64	96	64	96	64	96
p(t-test)	$2.19\text{x}10^{-1}(3.90\text{x}10^{-1})$		$9.51\text{x}10^{-1}(9.55\text{x}10^{-1})$		$5.28\text{x}10^{-2}(1.41\text{x}10^{-1})$		$2.93\text{x}10^{-1}(4.69\text{x}10^{-1})$	
p(Wilcoxon)	$3.09\text{x}10^{-1}(4.74\text{x}10^{-1})$		$5.74\text{x}10^{-1}(6.45\text{x}10^{-1})$		$5.25\text{x}10^{-2}(1.88\text{x}10^{-1})$		$2.83\text{x}10^{-2}(1.51\text{x}10^{-1})$	
Exon GC%	**30-40%**		**40-50%**		**50-60%**		**60-70%**	
Motif GC%	50	75	50	75	50	75	50	75
#Correlations	64	96	64	96	64	96	64	96
p(t-test)	$3.26\text{x}10^{-1}(4.75\text{x}10^{-1})$		$8.44\text{x}10^{-1}(9.55\text{x}10^{-1})$		$4.35\text{x}10^{-3}(1.39\text{x}10^{-2})$*		$4.50\text{x}10^{-1}(5.54\text{x}10^{-1})$	
p(Wilcoxon)	$2.47\text{x}10^{-1}(4.40\text{x}10^{-1})$		$5.43\text{x}10^{-1}(6.45\text{x}10^{-1})$		$6.11\text{x}10^{-3}(9.77\text{x}10^{-2})$		$9.15\text{x}10^{-1}(9.15\text{x}10^{-1})$	
Exon GC%	**30-40%**		**40-50%**		**50-60%**		**60-70%**	
Motif GC%	50	100	50	100	50	100	50	100
#Correlations	16	96	16	96	16	96	16	96
p(t-test)	$1.06\text{x}10^{-5}(1.69\text{x}10^{-4})$*		$3.16\text{x}10^{-3}(1.26\text{x}10^{-2})$*		$7.19\text{x}10^{-4}(5.75\text{x}10^{-3})$*		$6.88\text{x}10^{-2}(1.57\text{x}10^{-1})$	
p(Wilcoxon)	$2.62\text{x}10^{-2}(1.51\text{x}10^{-1})$		$7.03\text{x}10^{-2}(1.88\text{x}10^{-1})$		$6.27\text{x}10^{-2}(1.88\text{x}10^{-1})$		$1.79\text{x}10^{-1}(3.58\text{x}10^{-1})$	

Table 2.5: T-test and Wilcoxon-test comparisons of Pearson correlations for motif-pairs at 10bp spacing for varying motif GC and mean exon GC content in Mutant-r2 type *D. melanogaster*. FDR corrected p-values in parenthesis, using a False positive rate of 5% ($\alpha = 0.05$). * suggests rejection of the null hypothesis.

Motif spacing: **50bp**								
Exon GC%	**30-40%**		**40-50%**		**50-60%**		**60-70%**	
Motif GC%	50	0	50	0	50	0	50	0
#Correlations	16	96	16	96	16	96	13	96
p(t-test)	$9.09\text{x}10^{-1}(9.65\text{x}10^{-1})$		$8.87\text{x}10^{-1}(9.65\text{x}10^{-1})$		$2.40\text{x}10^{-1}(4.53\text{x}10^{-1})$		$9.65\text{x}10^{-1}(9.65\text{x}10^{-1})$	
p(Wilcoxon)	$8.79\text{x}10^{-2}(3.13\text{x}10^{-1})$		$5.35\text{x}10^{-1}(7.35\text{x}10^{-1})$		$1.79\text{x}10^{-1}(4.09\text{x}10^{-1})$		$8.07\text{x}10^{-1}(8.61\text{x}10^{-1})$	
Exon GC%	**30-40%**		**40-50%**		**50-60%**		**60-70%**	
Motif GC%	50	25	50	25	50	25	50	25
#Correlations	64	96	64	96	64	96	64	96
p(t-test)	$2.31\text{x}10^{-1}(4.53\text{x}10^{-1})$		$7.02\text{x}10^{-1}(8.99\text{x}10^{-1})$		$2.30\text{x}10^{-1}(4.53\text{x}10^{-1})$		$2.62\text{x}10^{-3}(2.02\text{x}10^{-2})$*	
p(Wilcoxon)	$4.85\text{x}10^{-2}(2.80\text{x}10^{-1})$		$2.11\text{x}10^{-1}(4.40\text{x}10^{-1})$		$1.11\text{x}10^{-1}(3.57\text{x}10^{-1})$		$1.63\text{x}10^{-3}(5.23\text{x}10^{-2})$	
Exon GC%	**30-40%**		**40-50%**		**50-60%**		**60-70%**	
Motif GC%	50	75	50	75	50	75	50	75
#Correlations	64	96	64	96	64	96	64	96
p(t-test)	$8.67\text{x}10^{-1}(9.65\text{x}10^{-1})$		$6.63\text{x}10^{-1}(8.85\text{x}10^{-1})$		$2.96\text{x}10^{-1}(4.99\text{x}10^{-1})$		$1.24\text{x}10^{-1}(3.98\text{x}10^{-1})$	
p(Wilcoxon)	$5.47\text{x}10^{-1}(7.35\text{x}10^{-1})$		$7.99\text{x}10^{-1}(8.61\text{x}10^{-1})$		$6.78\text{x}10^{-1}(7.75\text{x}10^{-1})$		$2.34\text{x}10^{-1}(4.40\text{x}10^{-1})$	
Exon GC%	**30-40%**		**40-50%**		**50-60%**		**60-70%**	
Motif GC%	50	100	50	100	50	100	50	100
#Correlations	16	96	16	96	16	96	16	96
p(t-test)	$4.76\text{x}10^{-2}(2.11\text{x}10^{-1})$		$6.06\text{x}10^{-1}(8.43\text{x}10^{-1})$		$1.42\text{x}10^{-1}(4.13\text{x}10^{-1})$		$2.07\text{x}10^{-1}(4.53\text{x}10^{-1})$	
p(Wilcoxon)	$6.42\text{x}10^{-1}(7.60\text{x}10^{-1})$		$9.59\text{x}10^{-1}(9.59\text{x}10^{-1})$		$1.63\text{x}10^{-1}(4.09\text{x}10^{-1})$		$2.34\text{x}10^{-1}(4.40\text{x}10^{-1})$	

Table 2.6: T-test and Wilcoxon-test comparisons of Pearson correlations for motif-pairs at 50bp spacing for varying motif GC and mean exon GC content in Mutant-r2 type *D. melanogaster*. FDR corrected p-values in parenthesis, using a False positive rate of 5% ($\alpha = 0.05$). * suggests rejection of the null hypothesis.

Motif spacing: **100bp**								
Exon GC%	**30-40%**		**40-50%**		**50-60%**		**60-70%**	
Motif GC%	50	0	50	0	50	0	50	0
#Correlations	16	96	16	96	16	96	15	96
p(t-test)	$7.05\text{x}10^{-1}(8.67\text{x}10^{-1})$		$1.84\text{x}10^{-1}(4.81\text{x}10^{-1})$		$4.86\text{x}10^{-1}(6.86\text{x}10^{-1})$		$2.26\text{x}10^{-1}(4.81\text{x}10^{-1})$	
p(Wilcoxon)	$7.56\text{x}10^{-1}(8.44\text{x}10^{-1})$		$1.63\text{x}10^{-1}(3.90\text{x}10^{-1})$		$4.69\text{x}10^{-1}(6.82\text{x}10^{-1})$		$1.06\text{x}10^{-2}(1.27\text{x}10^{-1})$	
Exon GC%	**30-40%**		**40-50%**		**50-60%**		**60-70%**	
Motif GC%	50	25	50	25	50	25	50	25
#Correlations	64	96	64	96	64	96	64	96
p(t-test)	$4.70\text{x}10^{-1}(6.86\text{x}10^{-1})$		$7.37\text{x}10^{-1}(8.85\text{x}10^{-1})$		$3.07\text{x}10^{-2}(1.47\text{x}10^{-1})$		$5.19\text{x}10^{-1}(7.12\text{x}10^{-1})$	
p(Wilcoxon)	$5.74\text{x}10^{-1}(7.07\text{x}10^{-1})$		$3.92\text{x}10^{-1}(6.07\text{x}10^{-1})$		$5.93\text{x}10^{-2}(2.73\text{x}10^{-1})$		$9.09\text{x}10^{-1}(9.34\text{x}10^{-1})$	
Exon GC%	**30-40%**		**40-50%**		**50-60%**		**60-70%**	
Motif GC%	50	75	50	75	50	75	50	75
#Correlations	64	96	64	96	64	96	64	96
p(t-test)	$2.98\text{x}10^{-1}(5.10\text{x}10^{-1})$		$5.60\text{x}10^{-3}(3.36\text{x}10^{-2})$*		$4.78\text{x}10^{-1}(6.86\text{x}10^{-1})$		$9.54\text{x}10^{-1}(9.65\text{x}10^{-1})$	
p(Wilcoxon)	$2.83\text{x}10^{-2}(1.94\text{x}10^{-1})$		$8.69\text{x}10^{-2}(3.01\text{x}10^{-1})$		$3.00\text{x}10^{-1}(5.12\text{x}10^{-1})$		$3.00\text{x}10^{-1}(5.12\text{x}10^{-1})$	
Exon GC%	**30-40%**		**40-50%**		**50-60%**		**60-70%**	
Motif GC%	50	100	50	100	50	100	50	100
#Correlations	16	96	16	96	16	96	16	96
p(t-test)	$8.31\text{x}10^{-3}(4.43\text{x}10^{-2})$*		$1.86\text{x}10^{-5}(4.47\text{x}10^{-4})$*		$2.92\text{x}10^{-1}(5.10\text{x}10^{-1})$		$1.10\text{x}10^{-1}(3.76\text{x}10^{-1})$	
p(Wilcoxon)	$1.09\text{x}10^{-1}(3.34\text{x}10^{-1})$		$4.46\text{x}10^{-3}(9.77\text{x}10^{-2})$		$4.69\text{x}10^{-1}(6.82\text{x}10^{-1})$		$1.63\text{x}10^{-1}(3.90\text{x}10^{-1})$	

Table 2.7: T-test and Wilcoxon-test comparisons of Pearson correlations for motif-pairs at 100bp spacing for varying motif GC and mean exon GC content in Mutant-r2 type *D. melanogaster*. FDR corrected p-values in parenthesis, using a False positive rate of 5% ($\alpha = 0.05$). * suggests rejection of the null hypothesis.

A

Wild-r2 *D. melanogaster*	
Parameter	Result
number of reads	13,072,176
number of mapped reads	13,072,176 (100%)
number of mapped bases	550,989,588 bp
number of sequenced bases	446,810,154 bp
mean mapping quality	138.2402
mean coverage data	3.2654X
std coverage data	76.6545X
Base composition / GC content	
Parameter	Result
number of A's	114,725,876 bp (25.68%)
number of C's	109,752,995 bp (24.56%)
number of T's	115,239,445 bp (25.79%)
number of G's	107,091,838 bp (23.97%)
number of N's	104,179,434 bp (23.32%)
GC percentage	48.53%

B

Mutant-r3 *D. melanogaster*	
Parameter	Result
number of reads	38,930,252
number of mapped reads	38,930,252 (100%)
number of mapped bases	5,216,530,413 bp
number of sequenced bases	1,728,910,071 bp
mean mapping quality	73.9482
mean coverage data	30.9152X
std coverage data	289.845X
Base composition / GC content	
Parameter	Result
number of A's	438,118,616 bp (25.34%)
number of C's	429,753,036 bp (24.86%)
number of T's	439,356,683 bp (25.41%)
number of G's	421,681,736 bp (24.39%)
number of N's	3,487,537,771 bp (201.72%)
GC percentage	49.25%

Table 2.8: BamQC analysis results for (A) wild-type-r2 and (B) mutant-r3 Drosophila.

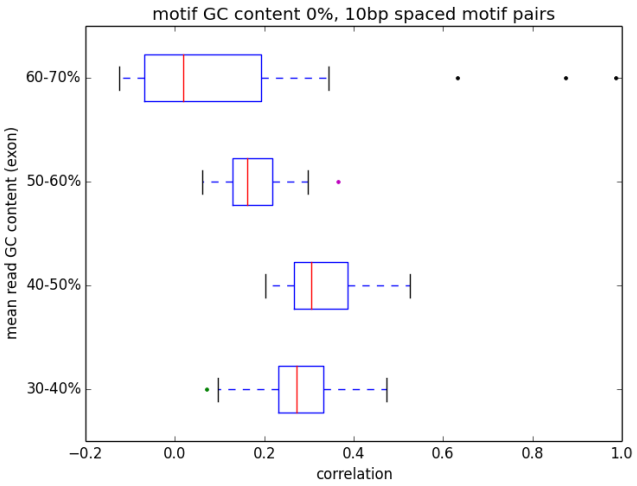

(a) Motif GC content of 0%

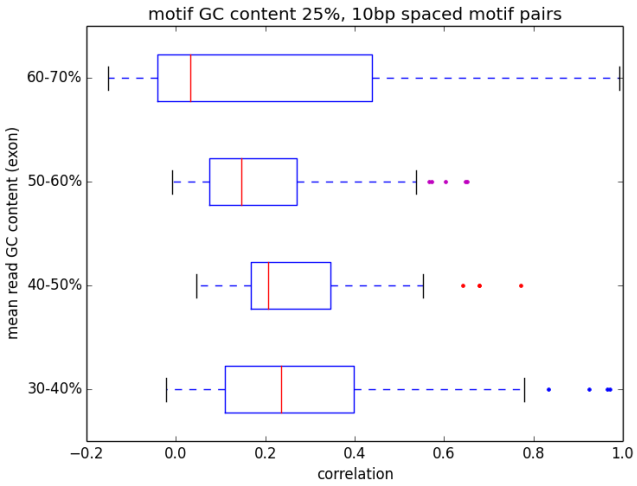

(b) Motif GC content of 25%

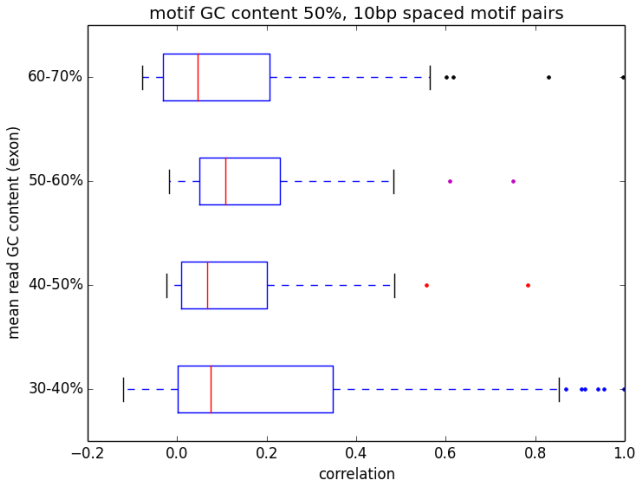

(c) Motif GC content of 50%

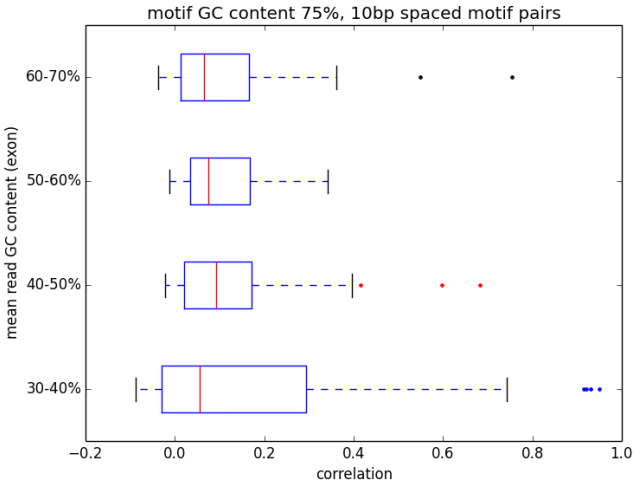

(d) Motif GC content of 75%

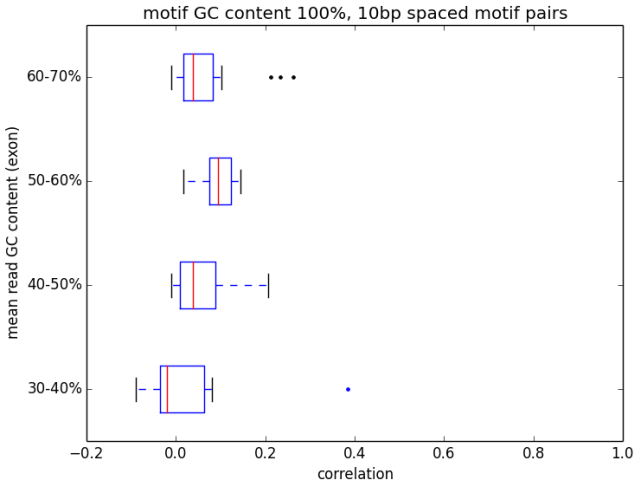

(e) Motif GC content of 100%

Figure 2.10: Box and whisker plots of motif-pair correlations at a distance of 10bp for Mutant-r2-type *D. melanogaster*

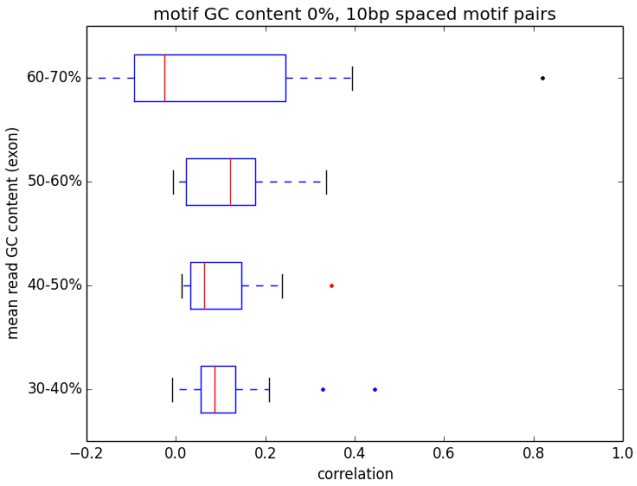

(a) Motif GC content of 0%

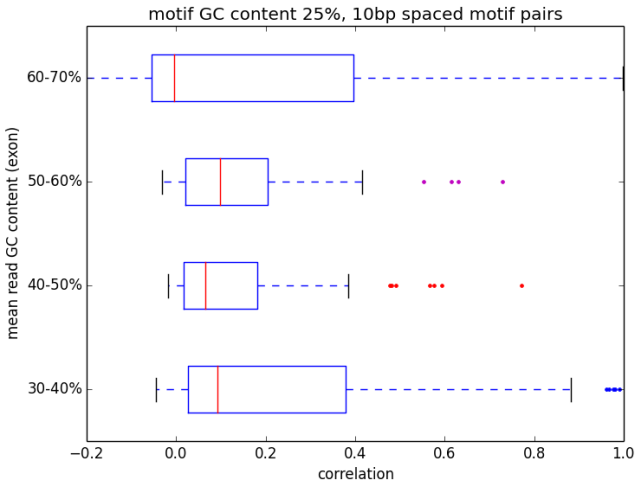

(b) Motif GC content of 25%

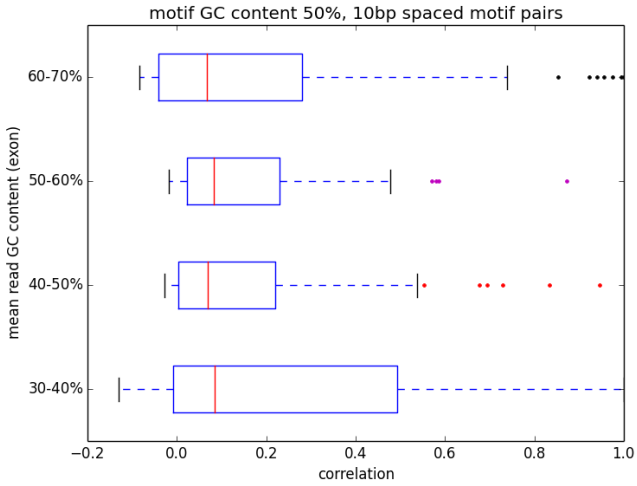

(c) Motif GC content of 50%

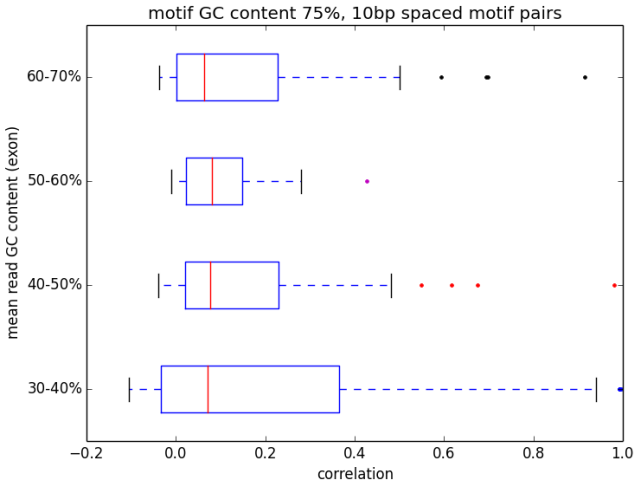

(d) Motif GC content of 75%

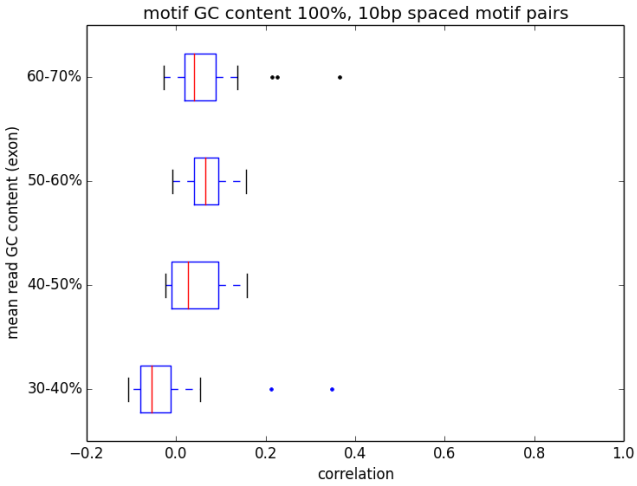

(e) Motif GC content of 100%

Figure 2.11: Box and whisker plots of motif pair correlations at a distance of 10bp for Mutant-r2-type *D. melanogaster* (Excluding hexamer regions)

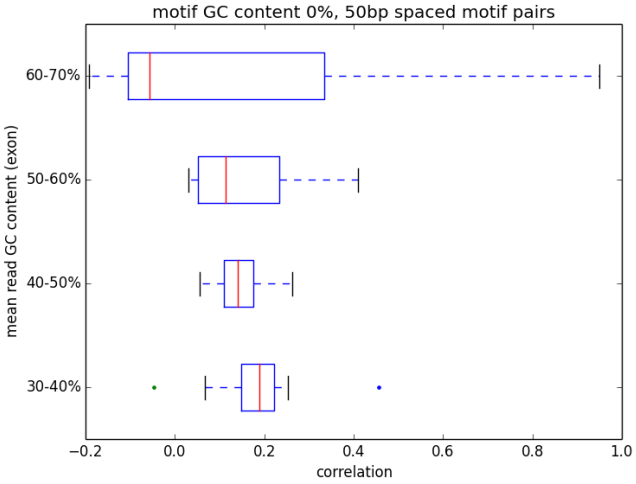

(a) Motif GC content of 0%

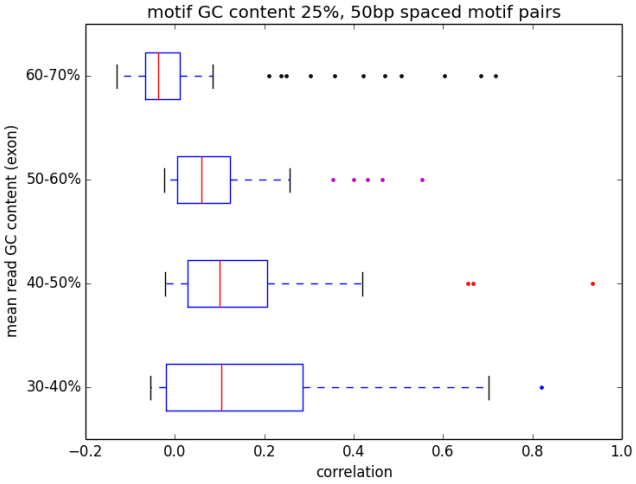

(b) Motif GC content of 25%

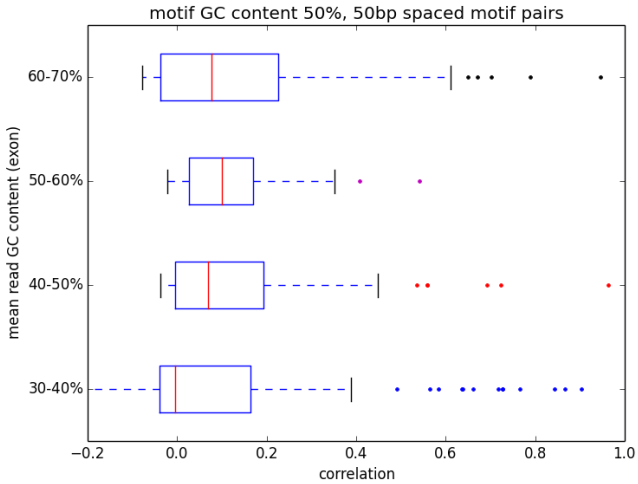

(c) Motif GC content of 50%

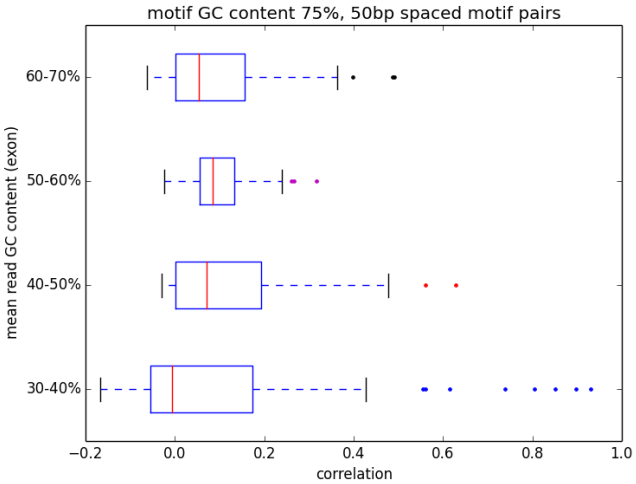

(d) Motif GC content of 75%

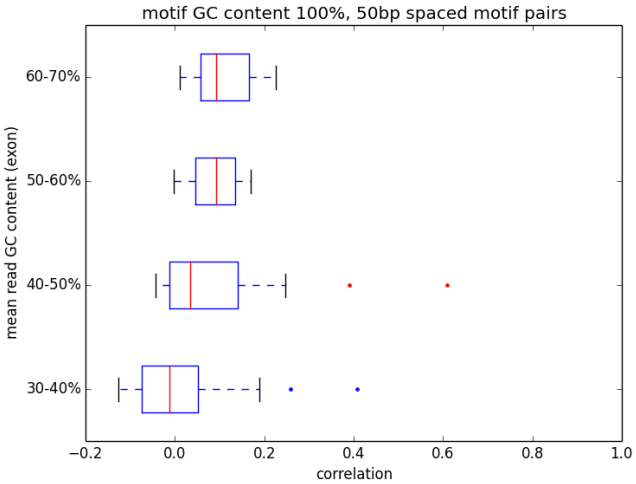

(e) Motif GC content of 100%

Figure 2.12: Box and whisker plots of motif-pair correlations at a distance of 50bp for Mutant-r2-type *D. melanogaster*

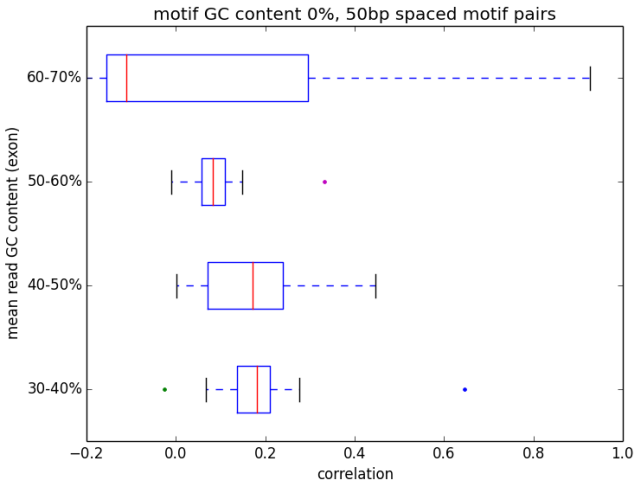

(a) Motif GC content of 0%

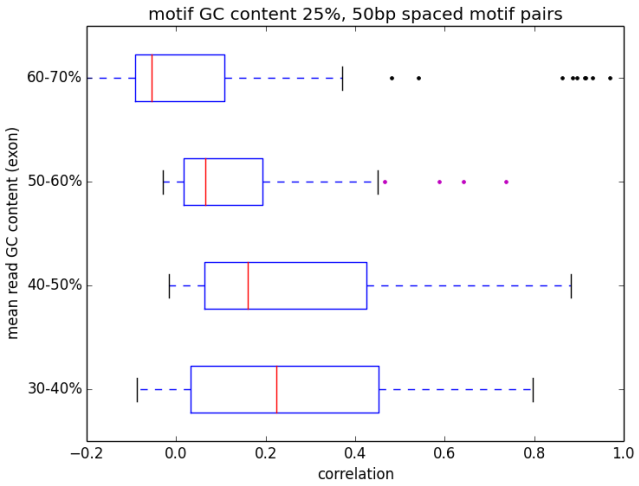

(b) Motif GC content of 25%

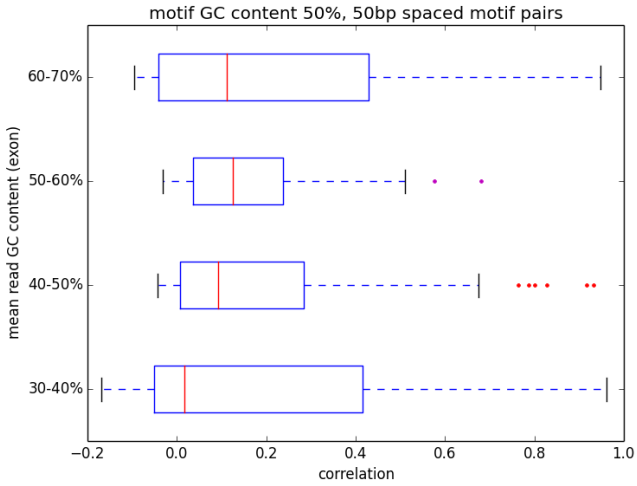

(c) Motif GC content of 50%

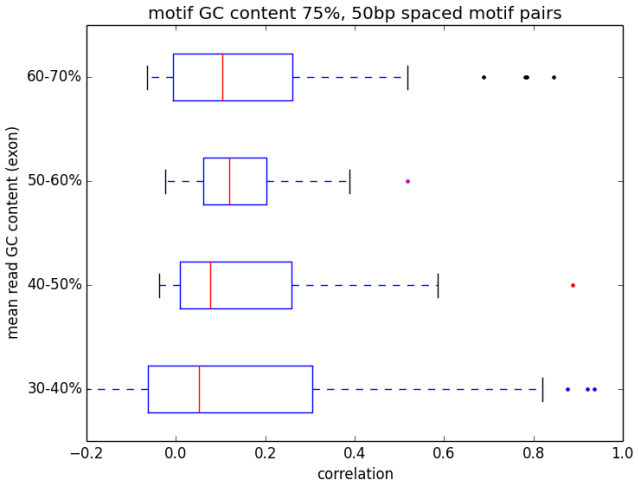

(d) Motif GC content of 75%

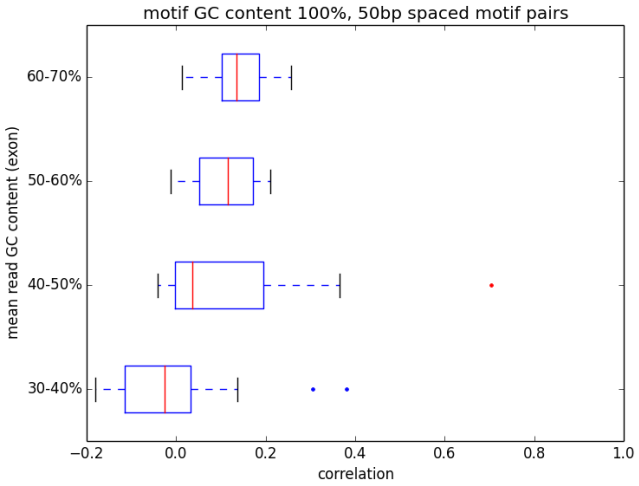

(e) Motif GC content of 100%

Figure 2.13: Box and whisker plots of motif pair correlations at a distance of 50bp for Mutant-r2-type *D. melanogaster* (Excluding hexamer regions)

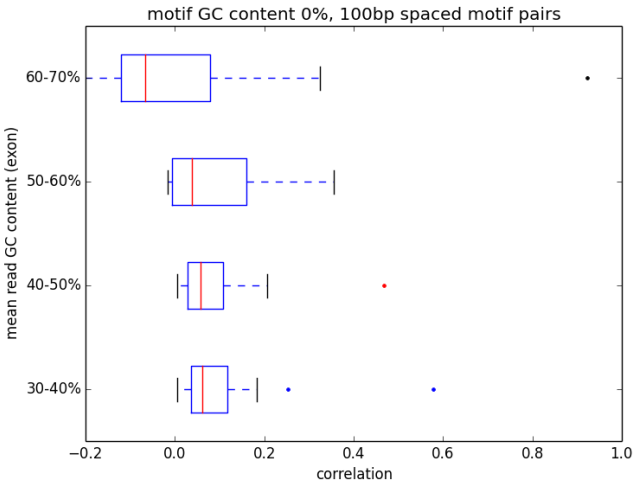

(a) Motif GC content of 0%

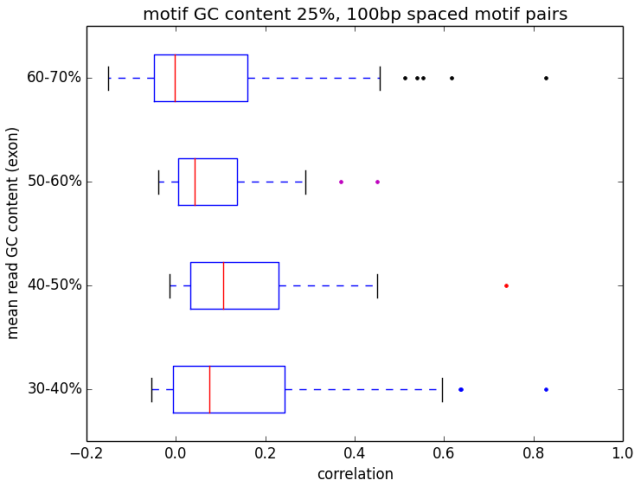

(b) Motif GC content of 25%

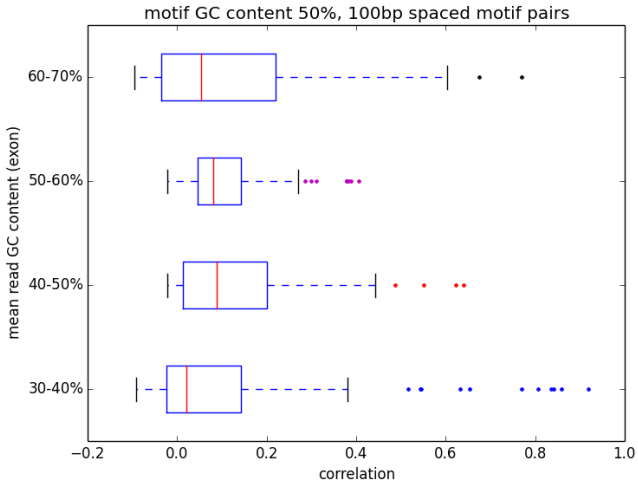

(c) Motif GC content of 50%

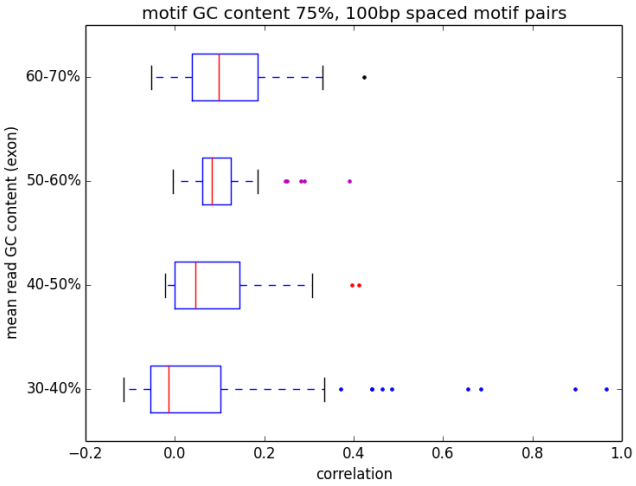

(d) Motif GC content of 75%

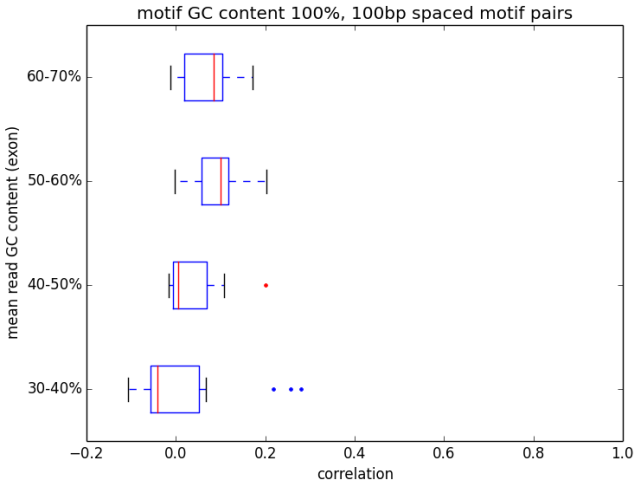

(e) Motif GC content of 100%

Figure 2.14: Box and whisker plots of motif-pair correlations at a distance of 100bp for Mutant-r2-type *D. melanogaster*.

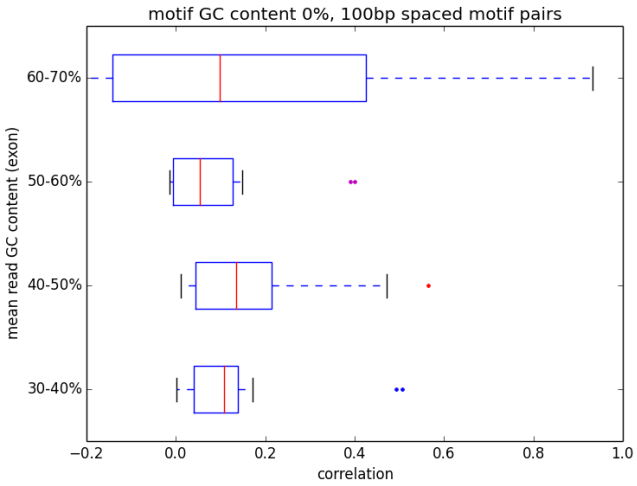

(a) Motif GC content of 0%

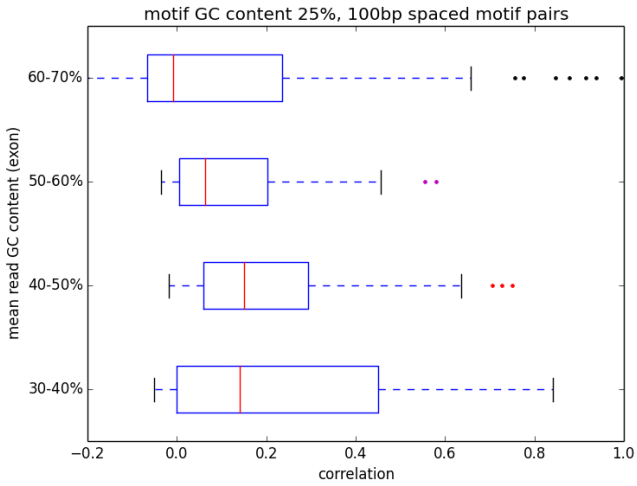

(b) Motif GC content of 25%

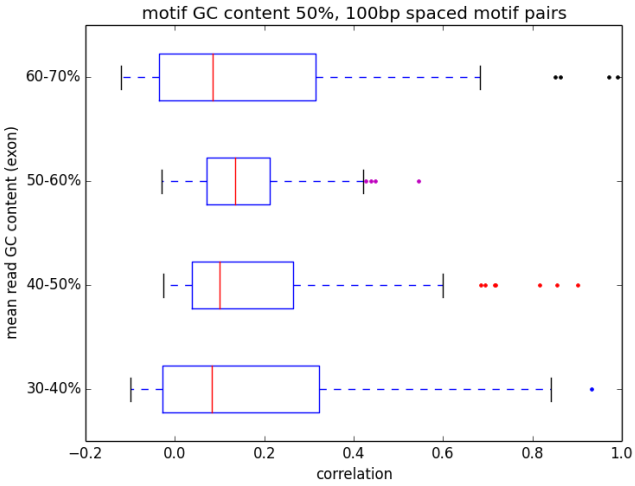

(c) Motif GC content of 50%

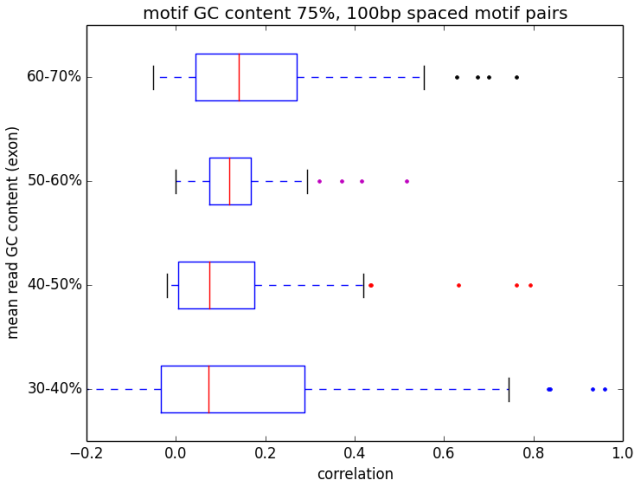

(d) Motif GC content of 75%

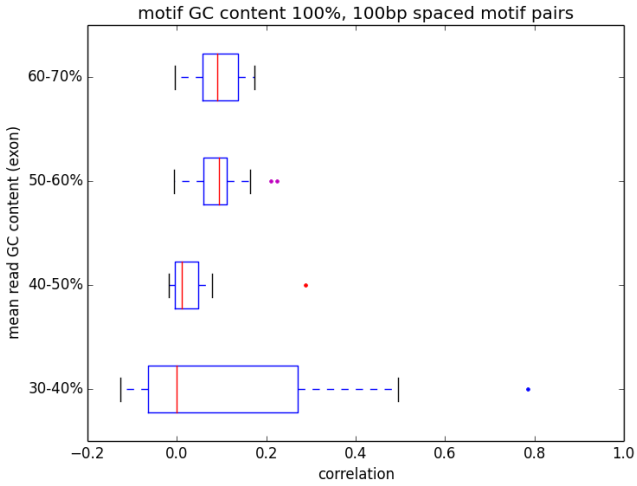

(e) Motif GC content of 100%

Figure 2.15: Box and whisker plots of motif pair correlations at a distance of 100bp for Mutant-r2-type *D. melanogaster* (Excluding hexamer regions)

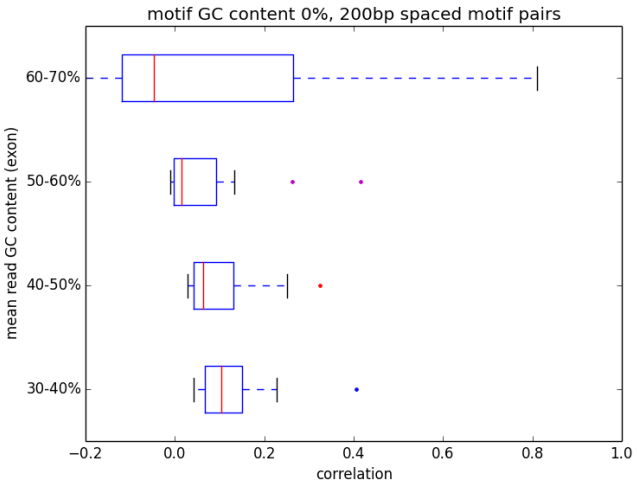

(a) Motif GC content of 0%

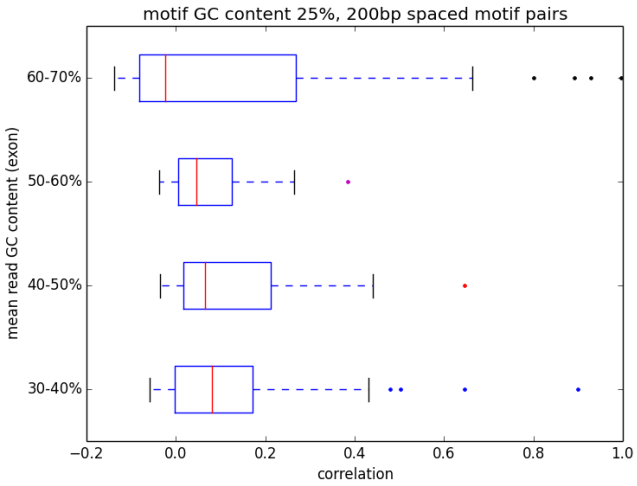

(b) Motif GC content of 25%

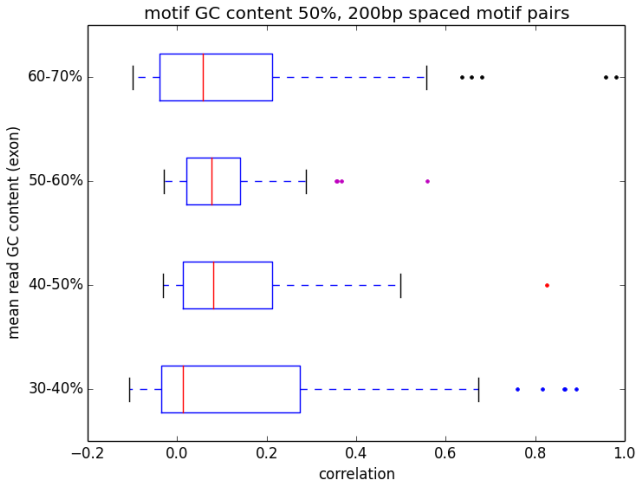

(c) Motif GC content of 50%

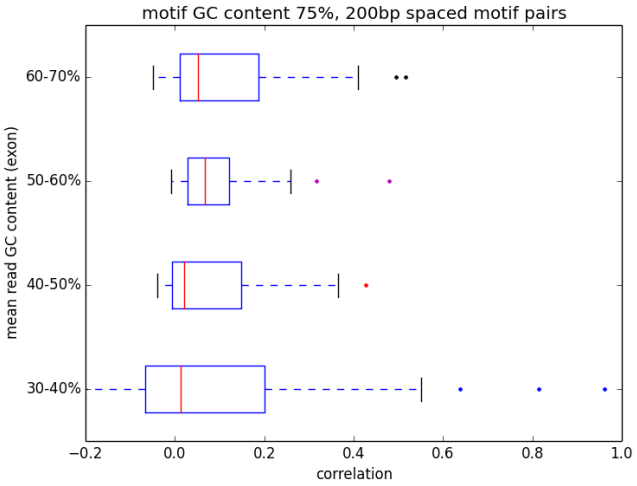

(d) Motif GC content of 75%

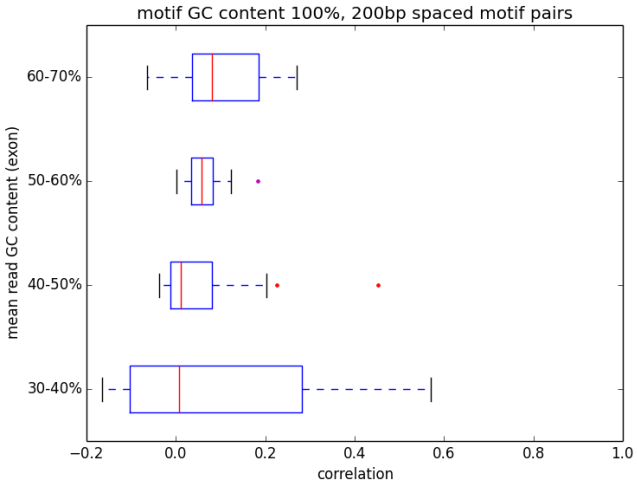

(e) Motif GC content of 100%

Figure 2.16: Box and whisker plots of motif-pair correlations at a distance of 200bp for Mutant-r2-type *D. melanogaster*.

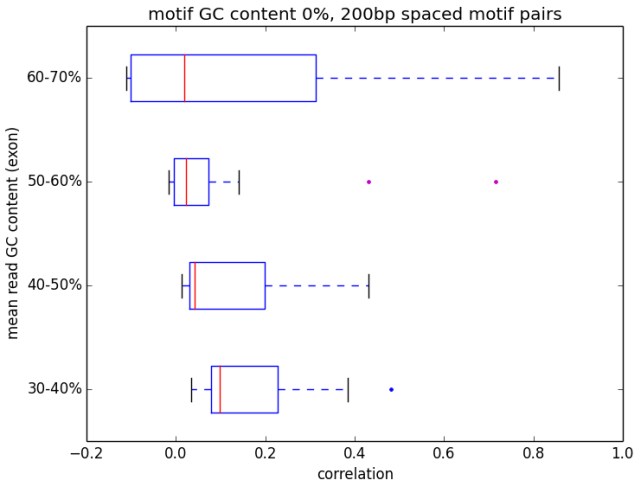

(a) Motif GC content of 0%

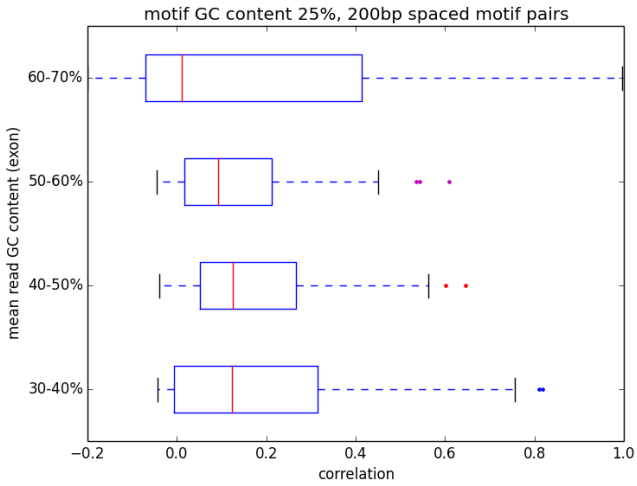

(b) Motif GC content of 25%

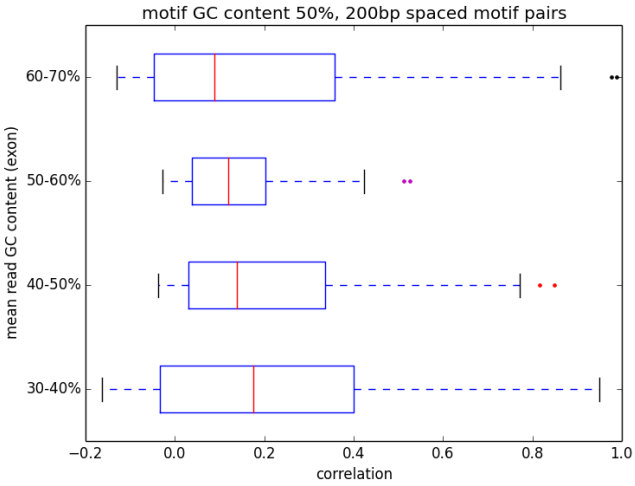

(c) Motif GC content of 50%

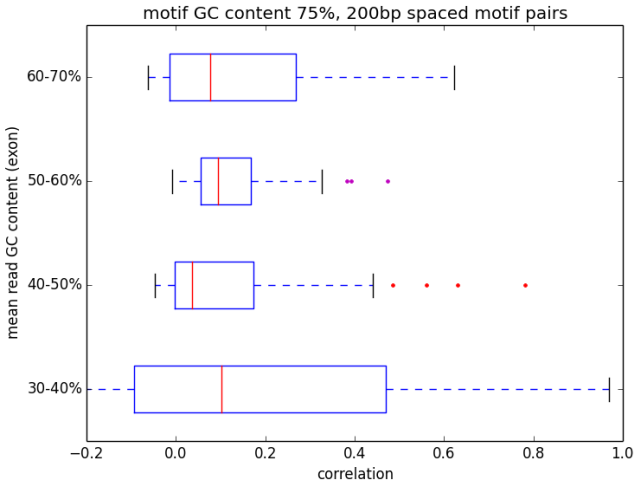

(d) Motif GC content of 75%

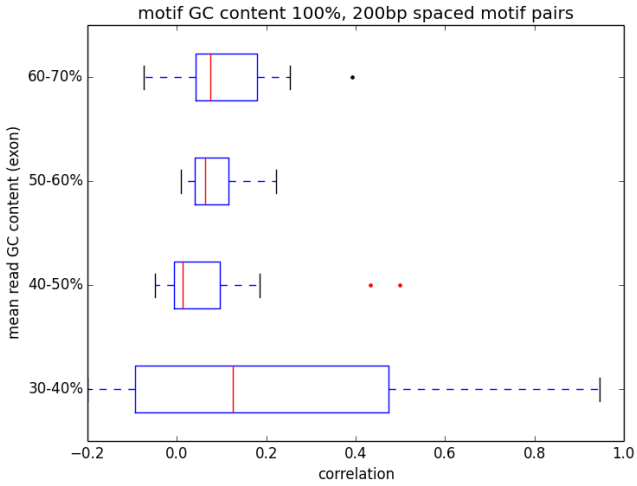

(e) Motif GC content of 100%

Figure 2.17: Box and whisker plots of motif pair correlations at a distance of 200bp for Mutant-r2-type *D. melanogaster*

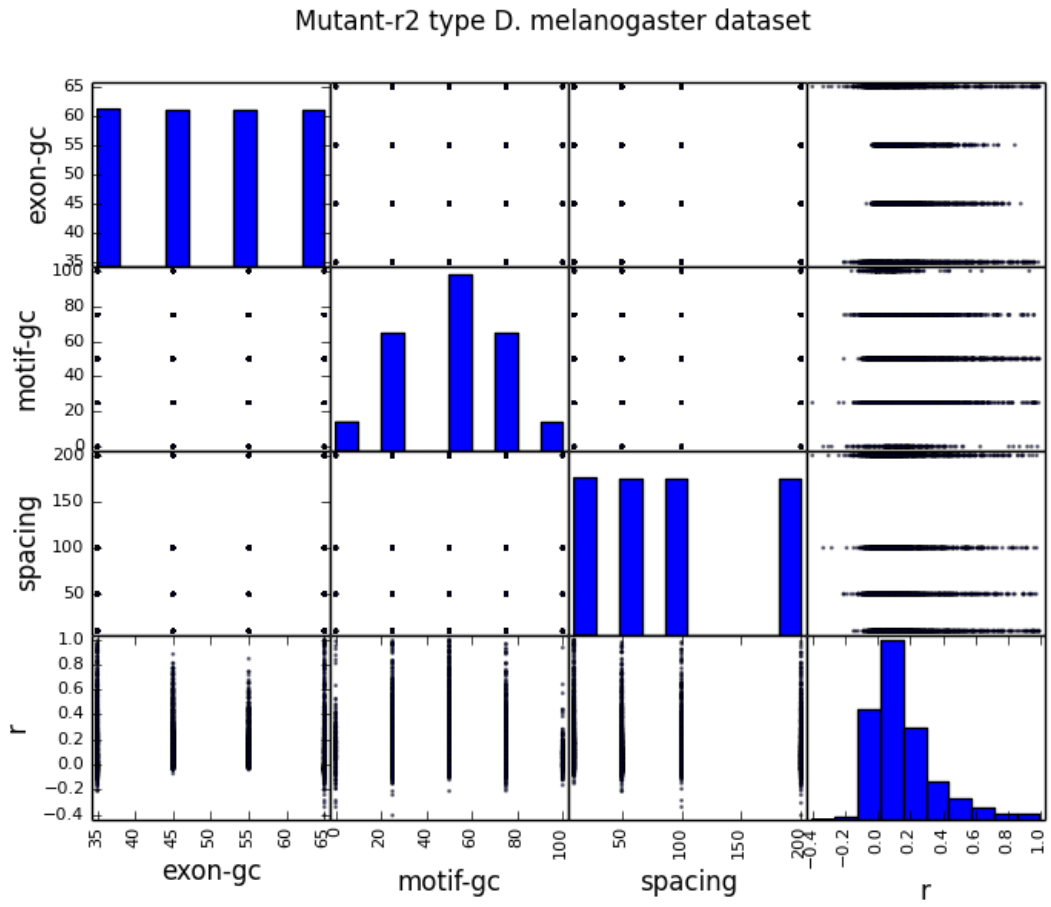

Figure 2.18: Scatter-matrix plot of correlation as a function of *4-mer* motif and exon GC content in mutant-r2 *D. melanogaster*.

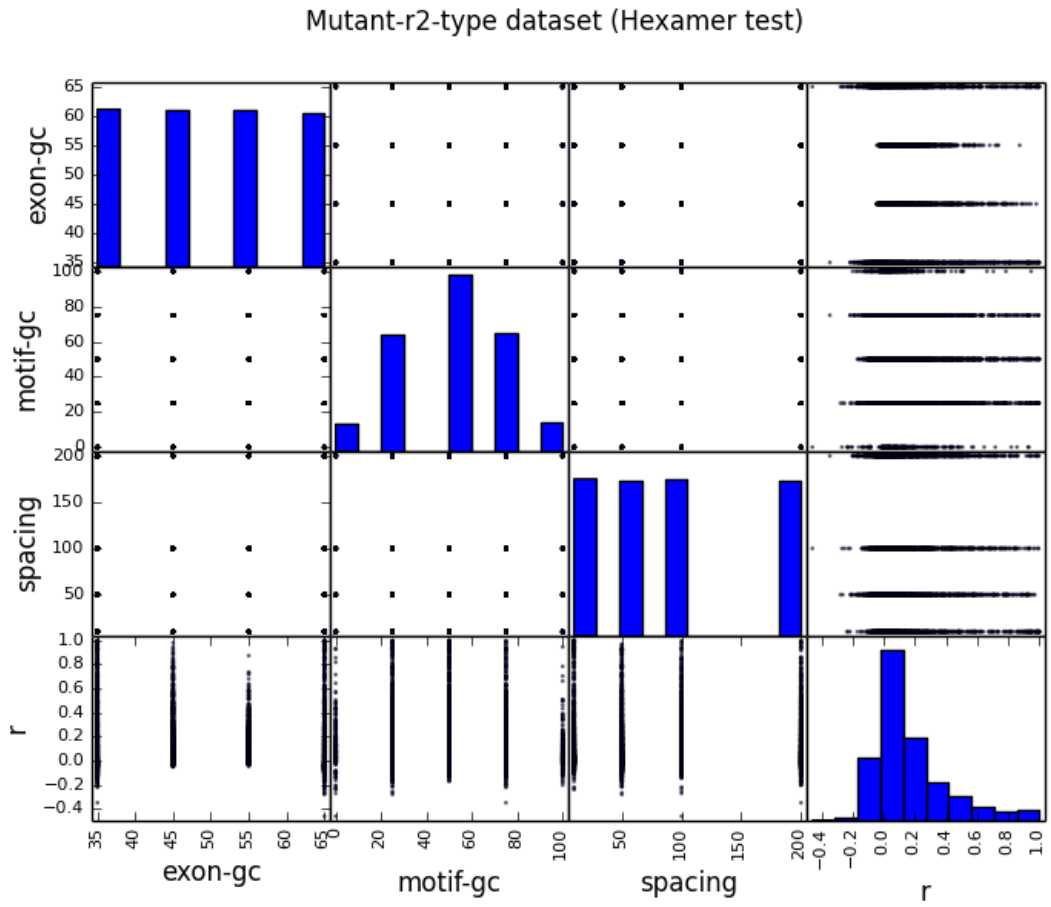

Figure 2.19: Scatter-matrix plot of correlation as a function of *4-mer* motif and exon GC content in mutant-r2 *D. melanogaster*. Random hexamer priming region has been excluded.

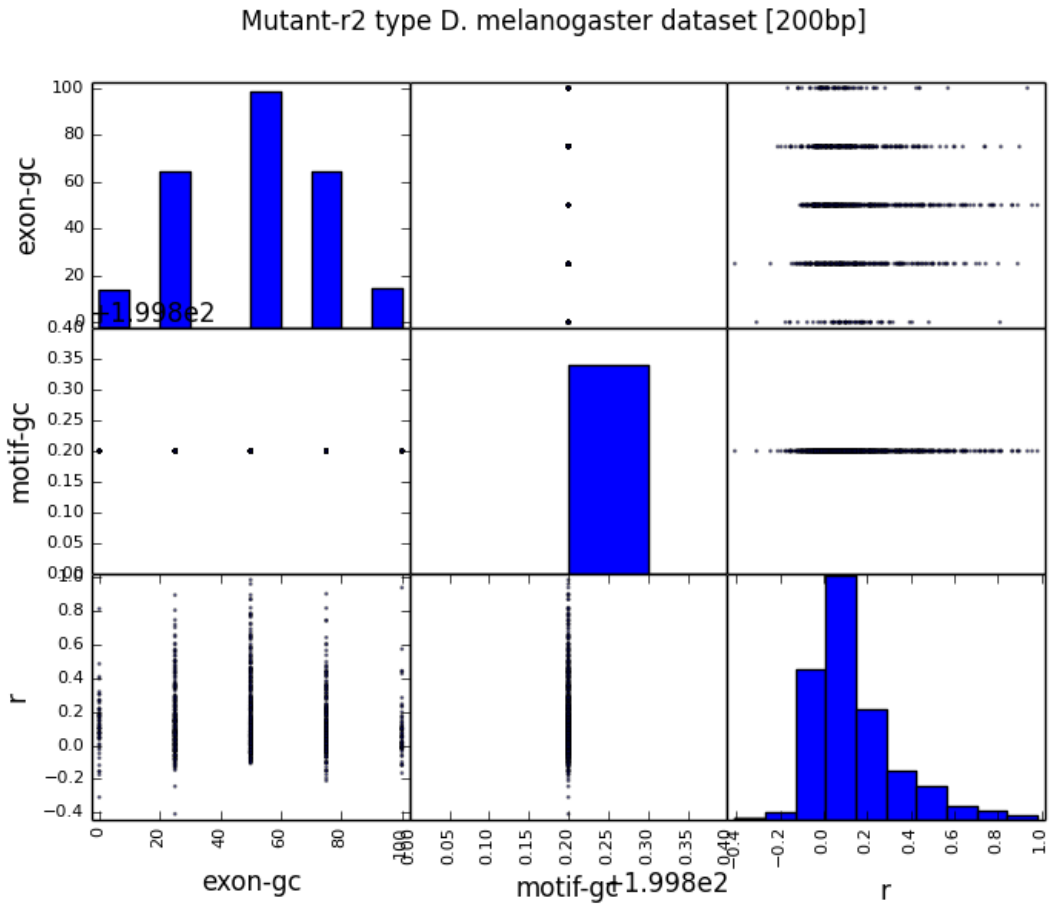

Figure 2.20: Scatter-matrix plot of correlation as a function of *4-mer* motif and exon GC content in mutant-r2 *D. melanogaster* at a motif-pair spacing of 200bp.